Journal of Sound and Vibration (2002) **255**(5), 931–963
doi:10.1006/jsvi.2001.4195, available online at http://www.idealibrary.com on IDEAL®

THE EFFECTS OF LARGE VIBRATION AMPLITUDES ON THE MODE SHAPES AND NATURAL FREQUENCIES OF THIN ELASTIC SHELLS. PART II: A NEW APPROACH FOR FREE TRANSVERSE CONSTRAINED VIBRATION OF CYLINDRICAL SHELLS

F. MOUSSAOUI

Faculté des Sciences et Techniques, Département de Physique, Laboratoire de Mécanique et Calcul Scientifique, BP. 509 Boutalamine, Errachidia, Morocco

R. BENAMAR

Ecole Mohammadia d'Ingénieurs, Département des E.G.T, Laboratoire d'Etude et de Recherche en Simulation Instrumentation et Mesures, BP. 765 Agdal, Rabat, Morocco. E-mail: rbenamar@emi.ac.ma

AND

R. G. WHITE

Department of Aeronautics and Astronautics, University of Southampton, Highfield Southampton, S017 1BJ, England

(*Received* 19 *April* 2001, *and in final form* 2 *November* 2001)

The non-linear dynamic behaviour of infinitely long circular cylindrical shells in the case of plane strains is examined and results are compared with previous studies. A theoretical model based on Hamilton's principle and spectral analysis previously developed for non-linear vibration of thin straight structures (beams and plates) is extended here to shell-type structures, reducing the large-amplitude free vibration problem to the solution of a set of non-linear algebraic equations. In the present work, the transverse displacement is assumed to be harmonic and is expanded in the form of a finite series of functions corresponding to the constrained vibrations, which exclude the axisymmetric displacements. The non-linear strain energy is expressed by taking into account the non-linear terms due to the considerable stretching of the shell middle surface induced by large deflections. It has been shown that the model presented here gives new results for infinitely long circular cylindrical shells and can lead to a good approximation for determining the fundamental longitudinal mode shape and the associated higher circumferencial mode shapes ($n > 3$) of simply supported circular cylindrical shells of finite length. The non-linear results at small vibration amplitudes are compared with linear experimental and theoretical results obtained by several authors for simply supported shells. Numerical results (non-linear frequencies, vibration amplitudes and basic function contributions) of infinite shells associated to the first four mode shapes of free vibrations, are obtained, using a multi-mode approach and are summarized in tables. Good agreement is found with results from previous studies for both small and large amplitudes of vibration. The non-linear mode shapes are plotted and discussed for different thickness to radius ratios. The distributions of the bending stresses associated with the mode shapes are given and compared with those obtained via the linear theory.

0022-460X/02/$35.00

1. INTRODUCTION

The subject of large vibration amplitudes of shell-type structures is a problem of great technical interest because it is encountered in many engineering applications, especially, in the aerospace industry and naval architecture. Geometrical non-linearity occurs very often in many applications of panels, particularly in aircraft. Aircraft skin-panels, especially those near the exhausts of jet engines, are often subject to high levels of acoustic pressure. This may result in large-amplitude, non-linear vibration of the panels [1–3]. It is known that when a shell is deflected more than approximately one-half of its thickness, significant geometrical non-linearity is induced [4]. Therefore, it is important to study such shells in order to determine their dynamic behaviour. At the beginning of this introduction, it may be interesting to note that shell vibration problems involve, even in the linear case, many specific difficulties. As outlined in reference [5], shell problems have the added complexity of curvature, compared with plates, which induces an eighth order system of governing partial differential equations of motion instead of the fourth order system obtained in the plate case and also the necessity of using a greater number of boundary conditions. On the other hand, shells are much more complicated than plates because all theoreticians agree on the form of the classical, fourth-order equations of motion for a plate, but such agreement does not exist in shell theory [5]. Numerous different shell theories have been derived and used in the literature [6–18].

The disagreements between these theories are due to the various assumptions made about the form of small terms and the order of terms which are retained in the analysis. In addition, some of the difficulties encountered are associated with the non-linear dynamic behaviour, such as those mentioned in reference [19], and with the numerical modelling of the geometrically non-linear vibration, which is not easy to take into account even in the case of simpler continuous systems, such as beams and plates [20–23].This is due, among many reasons, to the fact that the concept of normal modes becomes obscure in the non-linear case, since the assumptions of the time and space variable separation and that the motion is harmonic cannot be rigorously satisfied [21, 24]. For all of the above reasons, it clearly appears that studying the non-linear dynamic behaviour of shells may be a very difficult task which should be dealt with carefully and by means of successive approximations, each approximation having its corresponding domain of validity and being justified by the simplicity it introduces in the analysis and the ease with which it allows quantitative understanding of the shell dynamic behaviour and results to be obtained.

A variety of computational methods have been proposed and adopted by many researchers in the field of shell vibration modelling and analysis. The study of the dynamic behaviour of isotropic and orthotropic thin shells within the scope of linear models has been the subject of numerous works [25–33]. The free vibration of solid cylinders of different end supports [34] and of stress-free hollow cylinders of arbitrary cross-section [35] has been investigated by Liew *et al.* using a three-dimensional elasticity solution. The solution technique adopted in references [34, 35] has been extended by Hung *et al.* [36] to free vibration of cantilevered cylinders for different cross-sections and cavities. More recently, theoretical and numerical analyses of free vibration of solid cylinders having square and hexagonal cross-sections with combinations of fixed and free ends has been reported by Liew *et al.* [37]. A general review of the dynamic characteristics of shells has been given by Leissa in his monograph [5], and in a conference paper [19]. Recently, an excellent survey on vibration of shallow shells has been reported by Liew *et al.* reference [38] which summarizes papers published prior to 1996. This review paper documents recent developments in the free vibration analysis of thin, moderately thick, and thick shallow shells.

The first significant step towards the understanding and solution of non-linear vibration problems of shells has emanated from the work of Reissner in 1955 [39]. Specifically, for predominantly radial motion of shallow shells, Reissner showed that the mid-surface inertia terms can be neglected with a small resulting error. In this work, the authors are not concerned in giving a review on non-linear vibrations of shells. However, interested readers can turn to the recent survey of Amabili *et al.* [40] on non-linear vibration of closed cylindrical shells. Neglecting the tangential inertia terms and using Galerkin's procedure, Evensen showed that in the case of plane strains for an infinitely long circular cylindrical shell, the equations of motion reduce to the form of a Duffing equation [41, 42]. Radial displacements were assumed to be proportional to the fundamental mode and the contributions of the other modes were neglected but will be taken into account in this study (multi-mode approach).

Generally, dynamic analysis techniques applied to non-linear vibration problems can be more accurate if non-linear analytical methods are available. Considerable research has taken place on the non-linear dynamic behaviour of shells with large vibration amplitudes, based on different approximate methods. The most commonly used methods are the harmonic balance, the so-called method of averaging [24, 43, 44], Galerkin's method [39–41, 45–48], the perturbation method [45–47, 49], and the finite element method [4, 49, 50]. However, the majority of these works has been made based upon the single-mode approach and the contributions of other modes have been ignored.

Also, only a few papers are available which are concerned with the non-linear free vibration of shells of infinite length. Most of them are based on the single-mode approach [41, 42] and do not give any information concerning the form of the non-linear modes and their associated bending stress distributions. As accurate stress prediction is very important in engineering applications, it is necessary to investigate the non-linear behaviour of infinite shells in order to improve, qualitatively and quantitatively, the results obtained previously.

It appears from the brief review given above that in spite of considerable research, no general exact solution and systematic approach to the complicated problem of non-linear vibrations of shells is known which allows all or at least most of the known non-linear effects to be described in a unified manner. Furthermore, reliable, accurate results are generally lacking. Indeed, considerable disagreement among existing published results is found. The resulting knowledge in many cases is therefore, at best, only qualitative [19]. A theoretical model based on Hamilton's principle and spectral analysis has been proposed by Benamar *et al.* [20, 51] in order to adapt the Rayleigh–Ritz linear eigenvalue problem to non-linear problems of vibration of thin straight structures. This model was applied to simply supported, clamped beams, and to rectangular isotropic and laminated plates [21, 51–53]. This model was then extended in order to determine the first transverse non-linear mode shape of infinite cylindrical shells [54] and recently, has been applied, using a single-mode approach, to transverse non-linear vibration for finite circular cylindrical shells [55]. More recently, in Part I of this series of papers, the model was developed and applied to an infinite circular cylindrical shell taking into account the coupling between the circumferential and transverse mode shapes [56]. In a letter to the Editor [57], a criticism has been made by Amabili *et al.* concerning the form of the series used by Moussaoui *et al.* [56] to expand the transverse displacement function. In their reply [58], the authors have extensively discussed the purpose of the work presented in Part I [56], and the domain of application and validity of the assumptions made. In particular, it was specified that the work was concerned with: (1) free vibration, which justified the absence of the companion mode in the displacement function series used to express the shell response; (2) constrained vibration, which explains the absence of the axisymmetric functions in the series, and results in a considerable stretching of the shell mid-plane,

inducing the deformation of the shell mode shapes. More details concerning this discussion may be found in reference [58]. One purpose of the present paper (Part II) is to develop the work presented in references [41, 42, 54] in order to obtain reliable understanding of the non-linear dynamic behaviour, using a multi-mode approach (i.e., taking into account the contributions of the higher modes), of an infinite circular cylindrical shell when only the transverse displacement is considered. It is also intended to show that this special case of infinite shells can be useful to obtain, with a good approximation, the natural frequency of the lowest longitudinal mode, i.e., $m = 1$, and its associated higher circumferential modes for circular cylindrical shells of finite length. This approach simplifies strongly the formulation and the numerical effort for this shell category, compared with some previous approaches. For example, in references [27–29] the authors have used a laborious mathematical analysis in order to find the same results for the fundamental longitudinal mode ($m = 1$), which are obtained easily by the model presented here, as shown in section 3.8.

The simple mathematical model of shells based on the plane strain assumption used in references [41, 42, 54, 56] is adopted. This assumption changes the character of the shell motion from two-dimensional to one-dimensional and thus the analysis is considerably simplified. Assuming harmonic motion and expanding the transverse displacement in the form of a series of functions, the discretized expression for the non-linear strain energy at large vibration amplitudes is obtained. In this expression, in addition to the classical mass and rigidity tensors, a fourth order tensor appears due to the non-linearity. The technique adopted was to first assume a given value for one-mode contribution, and then apply Hamilton's principle in order to determine the other mode contributions. Minimization of the energy functional with respect to the unknown contribution coefficients leads to a set of non-linear algebraic equations which has been solved numerically in each case, to obtain a set of non-linear mode shapes (the study is extended here to the fourth circumferential mode), each mode being given as a function of the amplitude of vibration and the corresponding frequency. The numerical results obtained here are compared with those from previous studies and good agreement is found. The forms of the first four non-linear mode shapes and their corresponding bending stress distributions are represented and discussed for shells with various geometrical characteristics. This paper is organized as follows: in section 2 the analytical model and the formulation are stated. Then, detailed results concerning shells of infinite length are illustrated and discussed in section 3. A comparison of the results obtained here with both theoretical and experimental results given by several authors, for finite circular cylindrical shells, is presented in section 3.8.

2. MATHEMATICAL MODEL

2.1. BASIC ASSUMPTIONS

Consider the transverse vibration of the shell shown in Figure 1, having the following characteristics: E, Young's modulus, ρ the mass density, v the Poisson ratio, h thickness, R the radius of shell median surface and $W(y,t)$ the transverse displacement in the z direction. The basic assumptions considered in this work are as follows

(1) There is no motion in the direction of the length of the shell (plane strain assumption).
(2) As concern is only for free vibrational behaviour, the companion mode should be ignored.
(3) The case of constrained vibrations explains the absence of the axisymmetric terms in the expression of transverse displacement.

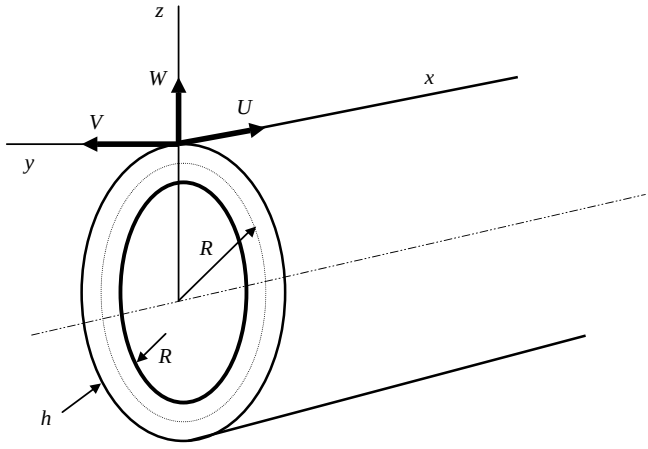

Figure 1. Schematic diagram of a circular cylindrical shell of infinite length.

(4) The transverse displacement $W(y,t)$ can be expressed in the form of a finite series in which the time and space variables are assumed to be separable as

$$W(y,t) = c_i w_i(y) \cos \omega t, \tag{1}$$

where c_i are the contribution coefficients of the basic functions w_i chosen in the present work as the shell linear mode shapes, with i varying from 1 to n, n being the number of functions.

(5) The cylindrical shell is very long (infinite length) and is vibrating in a mode so that the half-wavelength in the x direction is L. This may represent a finite shell of length L having a particular set of end conditions [41, 42]. This assumption implies that the displacement in the x-direction, u, equals 0 and terms involving derivatives with respect to x vanish. So, the strain tensor reduces to $\boldsymbol{\varepsilon}_y$ only, which is given by [56]

$$\boldsymbol{\varepsilon}_y = \partial V/\partial y + W/R + \tfrac{1}{2}(\partial W/\partial y)^2 + z(\partial^2 W/\partial y^2). \tag{2}$$

As the purpose of the present paper was to develop a simplified theory, facilitating easy derivation of many results previously given in the literature, based on the single-mode approach, via a laborious formulation and to obtain new more accurate results, based on a multi-mode approach, a simplification has been adopted in the above expression. This is based on the fact established in previous linear works [59, 60] according to which the nth transverse mode W_n and its associated circumferential mode V_n may be expressed by

$$W_n = c_n \cos(ny/R), \quad V_n = b_n \sin(ny/R) \tag{3a, b}$$

in which c_n and b_n are approximately related, as explained in Appendix A, by

$$c_n \approx -nb_n. \tag{4}$$

Substituting the W_n and V_n expressions given above in the first two terms of $\boldsymbol{\varepsilon}_y$ and taking into account the last relationship, a cancellation effect occurs, similar to that mentioned for plates by Han and Petyt [2], according to which

$$\partial V/\partial y + W/R = 0. \tag{5}$$

Substituting equation (5) into equation (2) leads to the expression of $\boldsymbol{\varepsilon}_y$ as

$$\boldsymbol{\varepsilon}_y = \tfrac{1}{2}(\partial W/\partial y)^2 + z(\partial^2 w/\partial y^2). \tag{6}$$

By using this simplification, and substituting in the total strain energy expression [38] of a shell having a unit length,

$$V = \frac{E}{2(1-\nu^2)} \int_{-h/2}^{h/2} \int_0^{2\pi R} (\boldsymbol{\varepsilon}^2 y)\, \mathrm{d}z\, \mathrm{d}y \tag{7}$$

leads to the strain energy as expressed in equation (8).

It should be noted that in Part I of this series of papers, a multi-mode approach has been adopted for both W and V and it was shown from the numerical solution of the set of non-linear algebraic equations that relationship (4) remains satisfied between the contributions c_n and b_n of the predominant function contributions at large vibration amplitudes. This justifies the adoption of assumption (5), based on equation (4), in the non-linear case.

On the other hand, in addition to the justification of expression (8) based on the nature of the infinite shell, the validity of the above approximate expression is discussed later in the light of the numerical results obtained (see section 3.3). It will be seen that the numerical results based on this expression obtained from the non-linear model developed here coincide exactly with the classical ones obtained by Evensen [41] and reported by Leissa [42] when only one mode is considered in the present model.

2.2. THE BENDING STRAIN, AXIAL STRAIN AND KINETIC ENERGIES OF A SHELL OF INFINITE LENGTH

Substituting expression (6) in Equation (7) and rearranging, the total strain can be written as the sum of two terms, the membrane strain energy V_m and the bending strain energy V_b as

$$V = V_m + V_b = \frac{3D}{2h^2} \int_0^{2\pi R} \left(\frac{\partial W}{\partial y}\right)^4 \mathrm{d}y + \frac{D}{2} \int_0^{2\pi R} \left(\frac{\partial^2 W}{\partial y^2}\right)^2 \mathrm{d}y. \tag{8}$$

where D is the bending stiffness given by $D = Eh^3/12(1-\nu^2)$. The membrane strain energy, V_m, induced by the considerable stretching of the shell middle surface is a fourth-order functional of W first derivative.

The kinetic energy of the shell is given by

$$T = \frac{\rho h}{2} \int_0^{2\pi R} \left(\frac{\partial W}{\partial t}\right)^2 \mathrm{d}y, \tag{9}$$

in which the longitudinal and tangential inertia terms are neglected, and ρ is the mass per unit volume.

2.3. DISCRETIZATION OF THE TOTAL STRAIN AND KINETIC ENERGY EXPRESSIONS

The discretization of total strain energy expression is made by substituting expression (1) into equation (8) and rearranging, leading to

$$V = \tfrac{1}{2} c_i c_j \mathbf{k}_{ij} \cos^2 \omega t + c_i c_j c_k c_l \mathbf{b}_{ijkl} \cos^4 \omega t. \tag{10}$$

Substituting equation (1) into Equation (9), the discretized expression of the kinetic energy is

$$T = \tfrac{1}{2}\omega^2 c_i c_j \mathbf{m}_{ij} \sin^2 \omega t \tag{11}$$

Non-dimensional formulation of the non-linear vibration problem can be made as. by putting

$$w_i(y) = h w_i^*(y/R) = h w^*{}_i(y^*), \quad \beta = h/R \tag{12}$$

where y^* is a non-dimensional co-ordinate; $y^* = y/R$.

One obtains

$$\frac{\mathbf{k}_{ij}}{\mathbf{k}_{ij}^*} = \frac{Eh^3}{(1-\nu^2)R}, \quad \frac{\mathbf{b}_{ijkl}}{\mathbf{b}_{ijkl}^*} = \frac{Eh^3}{(1-\nu^{21})R}, \quad \frac{\mathbf{m}_{ij}}{\mathbf{m}_{ij}^*} = \rho R h^3, \tag{13}$$

where $\mathbf{k}_{ij}^*$ is the non-dimensional general term of the classical rigidity tensor [**K**], given by

$$\mathbf{k}_{ij}^* = \frac{\beta^2}{12}\int_0^{2\pi} \frac{\partial^2 w_i^*}{\partial y^{*2}} \frac{\partial^2 w_j^*}{\partial y^{*2}}\, \mathrm{d}y^*. \tag{14}$$

$\mathbf{b}_{ijkl}^*$ is the non-dimensional general term of the fourth-order non-linear tensor [**B**], given by

$$\mathbf{b}_{ijkl}^* = \frac{\beta^2}{4}\int_0^{2\pi} \frac{\partial w_i^*}{\partial y^*} \frac{\partial w_j^*}{\partial y^*} \frac{\partial w_k^*}{\partial y^*} \frac{\partial w_l^*}{\partial y^*}\, \mathrm{d}y^* \tag{15}$$

and $\mathbf{m}_{ij}^*$ is the non-dimensional general term of the mass tensor [**M**], given by

$$\mathbf{m}_{ij}^* = \int_0^{2\pi} w_i^* w_j^*\, \mathrm{d}y^*. \tag{16}$$

2.4. FORMULATION OF ENERGY FUNCTIONAL AND GOVERNING EQUATIONS

The dynamic behaviour of the structure is governed by Hamilton's principle, which is symbolically written as

$$\delta \int_0^{2\pi/\omega} [V(t) - T(t)]\, \mathrm{d}t = 0. \tag{17}$$

Introducing assumed series (1) into energy condition (17) via equations (10) and (11) reduces the problem to that of finding the minimum of the function ϕ given by

$$\phi = \int_0^{2\pi/\omega} \left\{ \frac{Eh^3}{2(1-\nu^2)R} c_i c_j \mathbf{k}_{ij}^* \cos^2 \omega t + \frac{Eh^3}{2(1-\nu^2)} c_i c_j c_k c_l \mathbf{b}_{ijkl}^* / \cos^4 \omega t \right.$$
$$\left. - \tfrac{1}{2}\rho R h^3 \omega^2 c_i c_j \mathbf{m}_{ij}^* \sin^2 \omega t \right\} \mathrm{d}t \tag{18}$$

with respect to the undetermined constant c_i. Integrating the trigonometric functions $\cos^2 \omega t$, $\cos^4 \omega t$ and $\sin^2 \omega t$ over the range $[0, 2\pi/\omega]$ leads to the expression

$$\phi = (\pi/2\omega)\left[\frac{Eh^3}{(1-\nu^2)R} c_i c_j \mathbf{k}_{ij}^* + \frac{3}{4}\frac{Eh^3}{(1-\nu^2)R} c_i c_j c_k c_l \mathbf{b}_{ijkl}^* - \rho R h^3 \omega^2 c_i c_j \mathbf{m}_{ij}^* \right]. \tag{19}$$

In this expression, ϕ appears as a function of only the undetermined constants, c_i, $i = 1, \ldots, n$. Equation (17) reduces to

$$\partial\phi/\partial c_r = 0, \quad r = 1, \ldots, n. \tag{20}$$

Generally, the tensors $\mathbf{k}^*_{ij}$ and $\mathbf{m}^*_{ij}$ are symmetric, and the tensor $\mathbf{b}^*_{ijkl}$ is such that

$$\mathbf{b}^*_{ijkl} = \mathbf{b}^*_{klij}, \quad \mathbf{b}^*_{ijkl} = \mathbf{b}^*_{jikl}. \tag{21}$$

With these symmetry properties taken into account, it can be shown that equations (20) are equivalent to the following set of non-linear algebraic equations written in non-dimensional form as

$$c_i\mathbf{k}^*_{ir} + \tfrac{3}{2}c_ic_jc_k\mathbf{b}^*_{ijkr} - \omega^{*2}c_i\mathbf{m}^*_{ir} = 0, \quad r = 1, \ldots, n. \tag{22}$$

ω^{*2} is defined by equations (25) and (27). It can be seen that when the non-linear term is neglected, equation (22) reduces to the classical eigenvalue problem

$$[\mathbf{K}]\{\mathbf{C}\} = \omega^2[\mathbf{M}]\{\mathbf{C}\}, \tag{23}$$

which is the well-known Rayleigh–Ritz formulation of the linear vibration problem. In equation (23), $\{\mathbf{C}\} = [c_1 c_2, \ldots, c_n]^{\mathrm{T}}$ is the column matrix of coefficients.

2.5. METHOD OF SOLUTION

Equations (22) are a set of non-linear equations relating the n coefficients c_i and the frequency ω. So one has $(n + 1)$ unknowns and n equations. In order to complete the formulation, a further equation has to be added to equation (22). As no dissipation is considered here, such an equation can be obtained by the principle of conservation of energy, which can be written as [51]

$$V_{max} = T_{max}, \tag{24}$$

where V_{max} is the maximum value of the strain energy obtained from equation (10) for $t = 0$, which leads to $\cos^2\omega t = 1$, $\cos^4\omega t = 1$; and T_{max} is the maximum value of the kinetic energy obtained from equation (11) for $t = 2\pi/\omega$, i.e., $\sin^2\omega t = 1$. Equation (24) leads to the expression for ω^{*2}.

$$\omega^{*2} = (c_ic_j\mathbf{k}^*_{ij} + c_ic_jc_kc_l\mathbf{b}^*_{ijkl})/c_ic_j\mathbf{m}^*_{ij}. \tag{25}$$

The technique adopted in the present work was to apply condition (24) assuming a given value of the contribution c_{r0} of the function W_{r0}, and to determine the contribution of coefficients c_i $(i \neq r_0)$ of the functions w_i $(i \neq r_0)$. According to this, the r_0th non-linear transverse mode shape of the structure, corresponding to a given amplitude coefficient c_{r0}, is obtained by solving the set of $(n - 1)$ non-linear algebraic equations obtained by substituting expression (25) for ω^{*2} in equation (22), which leads to

$$c_i\mathbf{k}^*_{ir} + \tfrac{3}{2}c_ic_jc_k\mathbf{b}^*_{ijkr} - \frac{c_ic_j\mathbf{k}^*_{ij} + c_ic_jc_kc_l\mathbf{b}^*_{ijkl}}{c_ic_j\mathbf{m}^*_{ij}}c_i\mathbf{m}^*_{ir} = 0, \tag{26}$$

for $r \neq r_0$, and i, j, k and l varying from 1 to n.

The values of c_i, for $i \neq r_0$, obtained by solving equations (26) can be substituted into equation (25) to obtain the value of ω^{*2} corresponding to the chosen amplitude parameter c_{r0}. ω^{*2} is the non-dimensional non-linear natural frequency parameter related to the frequency parameter ω^2 by

$$\omega^2 = (12D/\rho R^2 h^3)\,\omega^{*2} = (E/\rho(1-\nu^2)\,R^2)\,\omega^{*2}. \tag{27}$$

This set of equations is identical to equation (17) established in references [21, 51, 52] for non-linear free vibration of fully clamped beams and rectangular plates. It has to be solved for each value of the shell thickness to radius ratio $\beta = h/R$ and assigned predominant function contribution, to obtain the amplitude-dependent non-linear shell mode shape.

As the shell considered is assumed to have an infinite length (see section 2.1), the basic functions used in the numerical model were independent of the length co-ordinate x^*. Thus, the transverse displacement functions are assumed to be

$$w_i^*(y^*) = \cos(iy^*) \quad \text{and} \quad u_i^* = 0, \quad v_i^* = 0. \tag{28}$$

2.6. BENDING STRESS EXPRESSIONS

To obtain the stress distribution along the shell circumferential co-ordinate, one considers the maximum bending strain ε_{yb} obtained for $z = h/2$ as

$$\varepsilon_{yb} = (h/2)(\partial^2 W/\partial y^2). \tag{29}$$

Using the classical thin shell assumption of plane strains and Hooke's law, the stresses can be written as

$$\sigma_{xb} = \frac{\nu hE}{2(1-\nu^2)}\frac{\partial^2 W}{\partial y^2}, \qquad \sigma_{yb} = \frac{hE}{2(1-\nu^2)}\frac{\partial^2 W}{\partial y^2}. \tag{30, 31}$$

In terms of the non-dimensional parameters defined in these equations, non-dimensional stresses σ_{xb}^* and σ_{yb}^* can be defined by

$$\sigma_{xb}^* = \nu(\partial^2 W^*/\partial y^{*2}), \qquad \sigma_{yb}^* = (\partial^2 W^*/\partial y^{*2}). \tag{32, 33}$$

The relationships between the dimensional and non-dimensional stresses are

$$\sigma = (E\beta^2/2(1-\nu^2))\,\sigma^*. \tag{34}$$

3. NUMERICAL RESULTS AND DISCUSSION

3.1. NUMERICAL DETAILS AND ITERATIVE PROCEDURE

To obtain the natural frequencies and the non-linear mode shapes of the shell described in section 2.1, 24 basic functions $(w_1^*, w_2^*, \ldots, w_{24}^*)$ associated with transverse displacement W^* were used. As a set of 23 non-linear algebraic equations had to be solved numerically for various values of the amplitudes of vibration and thickness to radius ratios, it was necessary to find an appropriate routine. The set of non-linear algebraic equations (26) has been solved numerically using the Harwell library routine NS01A. This routine is based on a hybrid iteration method combining the step descent and Newton's methods and does not

require a very good initial estimate of the solution [61]. In addition, a step calculation procedure, similar to that described in references [20, 21, 51, 52] and recently in references [54, 56], was adopted in order to facilitate convergence. So, for the rth non-linear mode shape, the first calculation was done in the neighbourhood of the linear solution by attributing a small numerical value to the coefficient c_r of the basic function w_r^*. The resulting solution was used as an initial estimate for the following step corresponding to $c + \Delta c$. Thus, by choosing in each case the convenient value of the step Δc, the rth non-linear mode shape has been calculated at various maximum vibration amplitude to shell thickness ratios extending up to a given value. This procedure has ensured rapid convergence when varying the amplitude. So, solutions have been obtained with quite a small number of iterations (for 12 equations one has an average of 30 for the first mode, 60 for the second mode, 67 for the third mode and 58 for the fourth mode).

3.2. CONVERGENCE OF THE SPECTRAL EXPANSION

Typical results referring to 24 basic functions $(w_1^*, w_2^*, \ldots, w_{24}^*)$, to a shell thickness to radius ratio equal to 0·05 and to three maximum values of the amplitude to thickness ratio are given in Table 1(a) for the first mode and in Table 1(b) for the second mode as an example. It can be seen that the only significant contributions are, as may be expected due to the antisymmetry of the first circumferential shell mode shape, those corresponding to the 12 first antisymmetric functions $(w_3^*, w_5^*, \ldots, w_{11}^*)$ in the y direction. Also, for the second mode, the only significant contributions are those corresponding to the 12 first symmetric functions $(w_4^*, w_6^*, \ldots, w_{12}^*)$ in the y direction. To check that the addition of symmetric shell functions does not affect the results, calculations were made with only 12 antisymmetric functions. The results show no significant change in both the value of the resonance frequency and the basic function contributions. It has been concluded that the non-linear mode shapes can be obtained with enough accuracy using the 12 first asymmetric basic functions, which simplify significantly the computational effort, since calculations of the non-linearity tensors b_{ijkl}^* involve $24^4 = 3{\cdot}31776 \times 10^5$ terms when using 24 basic functions, but only $12^4 = 2{\cdot}0736 \times 10^4$ terms when using 12 basic functions.

3.3. COMPARISON WITH PREVIOUS NON-LINEAR RESULTS

Unfortunately, the only results available in the literature concerning infinite shell vibration are based on the single-mode approach. So, although various techniques have been used, as discussed in the introduction, no results were found for the dependence of contribution coefficients on the amplitude of vibration. Therefore, the comparisons presented here have been restricted to the amplitude dependence of the resonance frequencies associated with the non-linear modes. The numerical results obtained from solution of the set of non-linear algebraic equations (26), for the four first non-linear mode, are compared in Table 2 and Figure 2(a, b) with theoretical results from the single-mode approach obtained by Evensen [41, 42] from application of the elliptic integral method to the temporal Duffing's differential equation. The plot shows clearly a hardening spring effect and the results are in good agreement with those obtained previously. The small discrepancy observed is due to the contribution of the higher modes at large vibration amplitudes (for the first mode one has $c_3, c_5, \ldots, c_{23}$ (see Table 3(a)); for the second mode $c_4, c_6, \ldots, c_{24}$ (see Table 3(b)) neglected in the Evensen theory, but taken into account in the present work. It may be also noted that this difference increases with increasing mode order.

TABLE 1

Typical numerical results obtained with 24 basic functions for $\beta = 0{\cdot}05$.

	(a) First non-linear mode			(b) Second non-linear mode		
W^*_{max}	0·05000489	1·29313848	2·65601182	0·04999912	1·29313827	2·65598944
ω^*_{nl}	0·01447428	0·02980875	0·05304729	0·05789714	0·11923500	0·21218956
c_1	0·5000000E − 01	0·1250000E + 01	0·2500000E + 01	0·5000000E − 01	0·1250000E + 01	0·2500000E + 01
c_2	− 0·34106394E − 06	0·49805060E − 09	0·86166030E − 11	− 0·56805119E − 05	− 0·99122924E − 11	− 0·44818521E − 14
c_3	0·51746515E − 05	0·39544554E − 01	0·12821332E + 00	− 0·33173742E − 06	0·98457468E − 11	0·51345876E − 13
c_4	0·51854558E − 07	0·10282707E − 09	0·28378750E − 11	− 0·12780645E − 06	0·66541415E − 08	0·11178721E − 04
c_5	0·35994557E − 08	0·32463606E − 02	0·21794811E − 01	− 0·76601710E − 08	0·83587146E − 11	− 0·32288541E − 14
c_6	− 0·20093295E − 08	0·18450919E − 10	0·20353644E − 11	0·52719613E − 05	0·39544553E − 01	0·12820898E + 00
c_7	− 0·32839247E − 09	0·31154854E − 03	0·46181939E − 02	− 0·38646661E − 08	− 0·67098760E − 11	− 0·18035535E − 13
c_8	− 0·37368853E − 09	− 0·28648901E − 11	0·12062785E − 11	− 0·50097398E − 08	0·58396248E − 08	0·97525561E − 05
c_9	− 0·10716825E − 09	0·32111575E − 04	0·10538398E − 02	− 0·22299828E − 09	0·47448442E − 11	0·13493355E − 13
c_{10}	− 0·19517440E − 09	0·47374060E − 11	− 0·42112540E − 12	0·97644259E − 09	0·32463589E − 02	0·21790737E − 01
c_{11}	− 0·82962388E − 10	0·34660765E − 05	0·25016077E − 03	0·34124614E − 09	− 0·10912219E − 11	0·10713121E − 13
c_{12}	− 0·26333067E − 09	− 0·29706443E − 11	0·38214036E − 12	− 0·19292243E − 08	0·81067301E − 08	0·94995427E − 05
c_{13}	0·64109074E − 09	0·38636377E − 06	0·61052232E − 04	− 0·17775408E − 08	0·10689132E − 11	0·17329868E − 14
c_{14}	− 0·71161678E − 09	− 0·95006180E − 12	0·10675514E − 12	− 0·11285825E − 09	0·31154585E − 03	0·46141755E − 02
c_{15}	0·46352492E − 09	0·44088210E − 07	0·15220703E − 04	0·13827008E − 08	− 0·37608352E − 12	0·33386785E − 14
c_{16}	0·34424202E − 09	− 0·20441423E − 11	0·28138018E − 12	0·17473280E − 08	0·17200508E − 07	0·11026143E − 04
c_{17}	0·25149266E − 09	0·51197250E − 08	0·38589934E − 05	0·64711228E − 09	0·16212013E − 11	0·71234741E − 14
c_{18}	0·82539031E − 09	− 0·80386666E − 13	− 0·19767430E − 12	− 0·28916257E − 10	0·32106037E − 04	0·10493563E − 02
c_{19}	− 0·11746653E − 08	0·60122584E − 09	0·99206000E − 06	0·18361815E − 08	0·82768236E − 12	0·44158086E − 14
c_{20}	0·22374112E − 09	0·90376169E − 13	− 0·55264592E − 13	− 0·42419465E − 09	0·48447886E − 07	0·15454427E − 04
c_{21}	0·46482131E − 09	0·72586837E − 10	0·25884886E − 06	− 0·98255288E − 09	− 0·18531141E − 11	− 0·85881300E − 14
c_{22}	0·14424362E − 09	0·95301553E − 12	− 0·12187053E − 12	0·15585320E − 08	0·34527498E − 05	0·24378983E − 03
c_{23}	− 0·29483433E − 09	0·94366184E − 11	0·70536193E − 07	− 0·98904878E − 09	0·13621540E − 12	0·31039621E − 14
c_{24}	0·14159019E − 09	0·46859115E − 12	− 0·28262307E − 13	0·26421053E − 09	0·16262372E − 06	0·25493788E − 04

TABLE 2

Comparison of frequency parameter of the first four mode shapes obtained for large vibration amplitudes, by the multi-mode approach, from the set of non ÷ linear algebraic equations (26) *with those obtained by Evensen using a single-mode approach, from the elliptic integral method.* [41, 42] $\beta = 0{\cdot}01$.

	First mode		Second mode		Third mode		Fourth mode	
C_i/h	$(\omega^*_{n1})^{\dagger}$	$(\omega^*_{n1})^{\ddagger}$	$(\omega^*_{n1})^{\ddagger}$	$(\omega^*_{n1})^{\ddagger}$	$(\omega^*_{n1})^{\ddagger}$	$(\omega^*_{n1})^{\ddagger}$	$(\omega^*_{n1})^{\ddagger}$	$(\omega^*_{n1})^{\ddagger}$
0·05	0·28949E − 02	0·28949E − 02	0·11579E − 01	0·11579E − 01	0·26054E − 01	0·26054E − 01	0·46318E − 01	0·46318E − 01
0·25	0·30831E − 02	0·30830E − 02	0·12332E − 01	0·12327E − 01	0·27747E − 01	0·27737E − 01	0·49329E − 01	0·49310E − 01
0·50	0·36084E − 02	0·35944E − 02	0·14434E − 01	0·14377E − 01	0·32476E − 01	0·32349E − 01	0·57735E − 01	0·57510E − 01
0·75	0·43451E − 02	0·42964E − 02	0·17381E − 01	0·17186E − 01	0·39106E − 01	0·38667E − 01	0·69522E − 01	0·68742E − 01
1·00	0·52042E − 02	0·51005E − 02	0·20817E − 01	0·20402E − 01	0·46837E − 01	0·45905E − 01	0·83267E − 01	0·81609E − 01
1·25	0·61343E − 02	0·59618E − 02	0·24537E − 01	0·23847E − 01	0·55209E − 01	0·53656E − 01	0·98150E − 01	0·95392E − 01
1·50	0·71078E − 02	0·68576E − 02	0·28431E − 01	0·27430E − 01	0·63970E − 01	0·61719E − 01	0·11372E + 00	0·10973E + 00
1·75	0·81090E − 02	0·77761E − 02	0·32436E − 01	0·31104E − 01	0·72981E − 01	0·69986E − 01	0·12974E + 00	0·12445E + 00
2·00	0·91287E − 02	0·87102E − 02	0·36515E − 01	0·34841E − 01	0·82158E − 01	0·78395E − 01	0·14606E + 00	0·13942E + 00
2·25	0·10161E − 01	0·96556E − 02	0·40646E − 01	0·38622E − 01	0·91453E − 01	0·86906E − 01	0·16258E + 00	0·15458E + 00
2·50	0·11204E − 01	0·10609E − 01	0·44814E − 01	0·42438E − 01	0·10083E + 00	0·95496E − 01	0·17926E + 00	0·16990E + 00
2·75	0·12253E − 01	0·11570E − 01	0·49011E − 01	0·46280E − 01	0·11027E + 00	0·10415E + 00	0·19604E + 00	0·18533E + 00
3·00	0·13307E − 01	0·12535E − 01	0·53229E − 01	0·50142E − 01	0·11977E + 00	0·11285E + 00	0·21292E + 00	0·20085E + 00
3·25	0·14366E − 01	0·13505E − 01	0·57464E − 01	0·54021E − 01	0·12929E + 00	0·12159E + 00	0·22986E + 00	0·21645E + 00
3·50	0·15428E − 01	0·14478E − 01	0·61712E − 01	0·57913E − 01	0·13885E + 00	0·13036E + 00	0·24685E + 00	0·23211E + 00
3·75	0·16493E − 01	0·15454E − 01	0·65970E − 01	0·61817E − 01	0·14843E + 00	0·13916E + 00	0·26388E + 00	0·24782E + 00
4·00	0·17559E − 01	0·16432E − 01	0·70238E − 01	0·65730E − 01	0·15803E + 00	0·14798E + 00	0·28095E + 00	0·26358E + 00
4·25	0·18628E − 01	0·17412E − 01	0·74512E − 01	0·69651E − 01	0·16765E + 00	0·15682E + 00	0·29805E + 00	0·27937E + 00
4·50	0·19698E − 01	0·18394E − 01	0·78793E − 01	0·73579E − 01	0·17728E + 00	0·16568E + 00	0·31517E + 00	0·29520E + 00
4·75	0·20770E − 01	0·10377E − 01	0·33079E − 01	0·77514E − 01	0·18693E + 00	0·17455E + 00	0·33232E + 00	0·31105E + 00
5·00	0·21842E − 01	0·20361E − 01	0·87369E − 01	0·81454E − 01	0·19658E + 00	0·18344E + 00	0·34948E + 00	0·32692E + 00

†Evensen·
‡present work

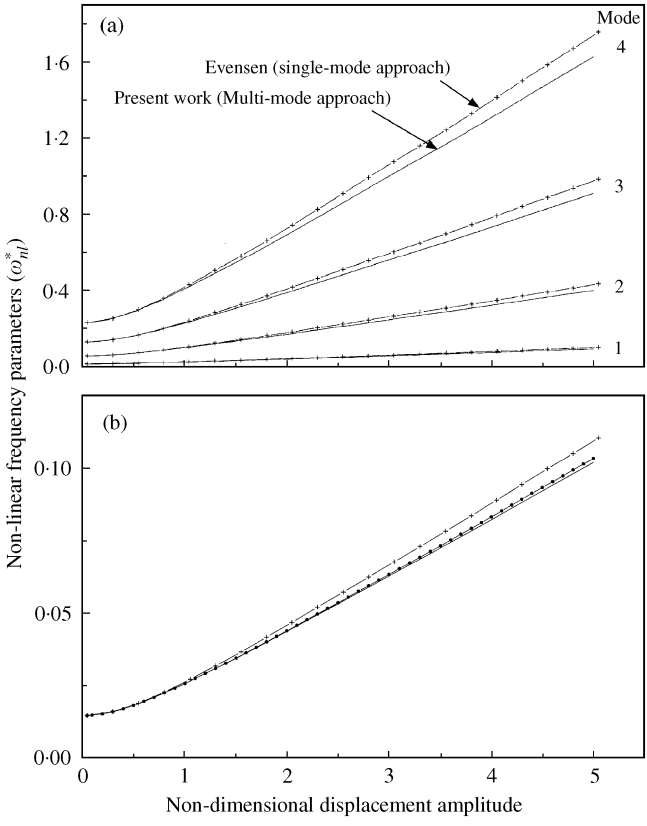

Figure 2. Comparison with previous (a) non-linear theoretical results and (b) previous theoretical results for the first mode 0 for $\beta = 0{\cdot}05$. Key for (a): ——, present work; - - + - -, Evensen single-mode approach: for (b) ——, Evensen single-mode approach; - - + - -, present work with three-function multi-mode approach; - - + - -, present work with 12-function multi-mode approach.

It is worth noticing that the solution obtained by Evensen and that obtained here for the 3-D case are very close and coincide exactly, as can be seen in Figure 2(b), when only one mode is considered in the present model.

3.4. GENERAL PRESENTATION OF THE NUMERICAL RESULTS

Numerical results for a circular cylindrical shell of infinite length having a thickness to radius ratio β equal to 0·05 are summarized in Table 3(a–d) for the first four mode shapes. In this table, c_i represents the contribution of the transverse basic functions and $(\omega^*_{nl}/\omega^*_l)_i$ represents the associated non-linear frequency ratios (where ω^*_l is the corresponding linear frequency parameter given in references [41, 42]). In Table 3(a), computed values of $c_3, c_5, \ldots, c_{23}$ corresponding to c_1 varying from 0·05 to 5 for the first mode are given with their associated non-linear frequency ratios $(\omega^*_{nl}/\omega^*_l)_1$. In Table 3(b), values of $c_4, c_6, \ldots, c_{24}$, corresponding to c_2 varying from 0·05 to 5 for the second mode, are presented with their associated non-linear frequency ratios $(\omega^*_{nl}/\omega^*_l)_2$. Table 3(c) contains the values of $c_1, c_5, c_7, \ldots, c_{23}$ corresponding to c_3 varying from 0·05 to 5 for the third mode and their associated non-linear frequency ratios $(\omega^*_{nl}/\omega^*_l)_3$. The values of $c_2, c_6, c_8, \ldots, c_{24}$

TABLE 3

Contribution coefficients of transverse basic functions corresponding to the first four non-linear mode shapes of an infinite shell having a thickness to radius ratio $\beta = 0{\cdot}05$

(a) First mode

ω_{nl}^*/ω_1^*	C_1	C_3	C_5	C_7	C_9	C_{11}	C_{13}	C_{15}	C_{17}	C_{19}	C_{21}	C_{23}
1·0028	0·05	0·52638E − 05	0·10761E − 08	0·38995E − 12	0·55429E − 13	0·48588E − 13	− 0·1222E − 13	0·29560E − 13	0·24242E − 14	0·13265E − 13	0·10482E − 13	0·38787E − 14
1·0676	0·25	0·63048E − 03	0·31209E − 05	0·18105E − 07	0·11402E − 09	0·75626E − 12	0·49206E − 14	0·58202E − 16	0·46557E − 16	0·79744E − 16	− 0·3046E − 16	0·18095E − 16
1·2451	0·50	0·44680E − 02	0·82748E − 04	0·17876E − 05	0·41851E − 07	0·10296E − 08	0·26187E − 10	0·68215E − 12	0·18067E − 13	0·46777E − 15	0·19652E − 16	0·44013E − 18
1·4883	0·75	0·12710E − 01	0·48024E − 03	0·21091E − 04	0·10012E − 05	0·49899E − 07	0·25707E − 08	0·13562E − 09	0·72833E − 11	0·39663E − 12	0·21841E − 13	0·12152E − 14
1·7669	1·00	0·24782E − 01	0·14804E − 02	0·10283E − 03	0·76947E − 05	0·60389E − 06	0·48971E − 07	0·40660E − 08	0·34367E − 09	0·29453E − 10	0·25530E − 11	0·22432E − 12
2·0652	1·25	0·39545E − 01	0·32464E − 02	0·31155E − 03	0·32112E − 04	0·34661E − 05	0·38636E − 06	0·44089E − 07	0·51211E − 08	0·60313E − 09	0·71841E − 10	0·87110E − 11
2·3755	1·50	0·55995E − 01	0·57925E − 02	0·70717E − 03	0·92525E − 04	0·12656E − 04	0·17864E − 05	0·25808E − 06	0·37947E − 07	0·56571E − 08	0·85322E − 09	0·13163E − 09
2·6937	1·75	0·73442E − 01	0·90382E − 02	0·13289E − 02	0·20925E − 03	0·34385E − 04	0·58260E − 05	0·10099E − 05	0·17816E − 06	0·31864E − 07	0·57685E − 08	0·10739E − 08
3·0173	2·00	0·91451E − 01	0·12865E − 01	0·21924E − 02	0·40038E − 03	0·76190E − 04	0·14935E − 04	0·29940E − 05	0·61066E − 06	0·12628E − 06	0·26452E − 07	0·57288E − 08
3·3448	2·25	0·10976E + 00	0·17152E − 01	0·32942E − 02	0·67927E − 03	0·14580E − 03	0·32203E − 04	0·72703E − 05	0·16696E − 05	0·38877E − 06	0·91777E − 07	0·22518E − 07
3·6752	2·50	0·12821E + 00	0·21795E − 01	0·46182E − 02	0·10538E − 02	0·25016E − 03	0·61052E − 04	0·15221E − 04	0·38590E − 05	0·99206E − 06	0·25885E − 06	0·70536E − 07
4·0079	2·75	0·14672E + 00	0·26706E − 01	0·61419E − 02	0·15270E − 02	0·39488E − 03	0·10490E − 03	0·28451E − 04	0·78450E − 05	0·21936E − 05	0·62326E − 06	0·18576E − 06
4·3424	3·00	0·16523E + 00	0·31816E − 01	0·78403E − 02	0·20976E − 02	0·58396E − 03	0·16690E − 03	0·48672E − 04	0·14426E − 04	0·43365E − 05	0·13262E − 05	0·42712E − 06
4·6783	3·25	0·18371E + 00	0·37075E − 01	0·96886E − 02	0·27616E − 02	0·81981E − 03	0·24974E − 03	0·77583E − 04	0·24489E − 04	0·78410E − 05	0·25575E − 05	0·88134E − 06
5·0153	3·50	0·20215E + 00	0·42441E − 01	0·11664E − 01	0·35131E − 02	0·11034E − 02	0·35555E − 03	0·11678E − 03	0·38964E − 04	0·13189E − 04	0·45536E − 05	0·16657E − 05
5·3533	3·75	0·22053E + 00	0·47884E − 01	0·13746E − 01	0·43452E − 02	0·14345E − 02	0·48590E − 03	0·16770E − 03	0·58777E − 04	0·20906E − 04	0·75928E − 05	0·29285E − 05
5·6922	4·00	0·23886E + 00	0·53382E − 01	0·15917E − 01	0·52505E − 02	0·18120E − 02	0·64177E − 03	0·23154E − 03	0·84818E − 04	0·31537E − 04	0·11987E − 04	0·48474E − 05
6·0317	4·25	0·25713E + 00	0·58918E − 01	0·18161E − 01	0·62216E − 02	0·22341E − 02	0·82365E − 03	0·30929E − 03	0·11791E − 03	0·45634E − 04	0·18073E − 04	0·76259E − 05
6·3718	4·50	0·27534E + 00	0·64480E − 01	0·20465E − 01	0·72513E − 02	0·26985E − 02	0·10316E − 02	0·40168E − 03	0·15877E − 03	0·63733E − 04	0·26203E − 04	0·11489E − 04
6·7124	4·75	0·29350E + 00	0·70056E − 01	0·22820E − 01	0·83330E − 02	0·32025E − 02	0·12653E − 02	0·50925E − 03	0·20806E − 03	0·86345E − 04	0·36732E − 04	0·16675E − 04
7·0534	5·00	0·31161E + 00	0·75642E − 01	0·25215E − 01	0·94604E − 02	0·37436E − 02	0·15243E − 02	0·63230E − 03	0·26628E − 03	0·11394E − 03	0·50014E − 04	0·23435E − 04

TABLE 3

Continued

(b) Second mode

ω_{n1}^*/ω_1^*	C_2	C_4	C_6	C_8	C_{10}	C_{12}	C_{14}	C_{16}	C_{18}	C_{20}	C_{22}	C_{24}
1·0028	0·05	0·13830E − 09	0·52638E − 05	0·17321E − 11	0·10671E − 08	0·28125E − 12	0·84018E − 13	− 0·1960E − 13	0·90944E − 13	− 0·4160E − 13	− 0·33822E − 13	− 0·8478E − 13
1·0676	0·25	0·32064E − 14	0·63048E − 03	0·55909E − 16	0·31209E − 05	0·97624E − 17	0·18105E − 07	0·33855E − 16	0·11403E − 09	0·36953E − 16	0·75490E − 12	0·21843E − 14
1·2451	0·50	− 0·29989E − 13	0·44680E − 02	0·12903E − 16	0·82748E − 04	0·73428E − 14	0·17876E − 05	0·65023E − 13	0·41851E − 07	0·77602E − 12	0·10294E − 08	0·11081E − 10
1·4883	0·75	0·20267E − 11	0·12710E − 01	0·22461E − 11	0·48024E − 03	0·58564E − 11	0·21091E − 04	0·25695E − 10	0·10011E − 05	0·15285E − 09	0·49863E − 07	0·10860E − 08
1·7669	1·00	0·25003E − 09	0·24782E − 01	0·23557E − 09	0·14804E − 02	0·41603E − 09	0·10283E − 03	0·11848E − 08	0·76943E − 05	0·45289E − 08	0·60274E − 06	0·20651E − 07
2·0652	1·25	0·66493E − 08	0·39545E − 01	0·58401E − 08	0·32464E − 02	0·81047E − 08	0·31155E − 03	0·17202E − 07	0·32106E − 04	0·48448E − 07	0·34528E − 05	0·16262E − 06
2·3755	1·50	0·70146E − 07	0·55995E − 01	0·60142E − 07	0·57925E − 02	0·71893E − 07	0·70714E − 03	0·12392E − 06	0·92483E − 04	0·27946E − 06	0·12572E − 04	0·75055E − 06
2·6937	1·75	0·40880E − 06	0·73442E − 01	0·34909E − 06	0·90381E − 02	0·38051E − 06	0·13288E − 02	0·56456E − 06	0·20905E − 03	0·10769E − 05	0·34035E − 04	0·24436E − 05
3·0173	2·00	0·15942E − 05	0·91450E − 01	0·13675E − 05	0·12864E − 01	0·14082E − 05	0·21919E − 02	0·18739E − 05	0·39969E − 03	0·31422E − 05	0·75082E − 04	0·62545E − 05
3·3448	2·25	0·46818E − 05	0·10976E + 00	0·40480E − 05	0·17151E − 01	0·40261E − 05	0·32926E − 02	0·49500E − 05	0·67737E − 03	0·75070E − 05	0·14293E − 03	0·13466E − 04
3·6752	2·50	0·11179E − 04	0·12821E + 00	0·97526E − 05	0·21791E − 01	0·94995E − 05	0·46142E − 02	0·11026E − 04	0·10494E − 02	0·15454E − 04	0·24379E − 03	0·25494E − 04
4·0079	2·75	0·22853E − 04	0·14671E + 00	0·20117E − 04	0·26697E − 01	0·19360E − 04	0·61332E − 02	0·21550E − 04	0·15177E − 02	0·28388E − 04	0·38230E − 03	0·43737E − 04
4·3424	3·00	0·41471E − 04	0·16521E + 00	0·36817E − 04	0·31799E − 01	0·35204E − 04	0·78236E − 02	0·38012E − 04	0·20803E − 02	0·47685E − 04	0·56132E − 03	0·69460E − 04
4·6783	3·25	0·68557E − 04	0·18368E + 00	0·61345E − 04	0·37043E − 01	0·58490E − 04	0·95594E − 02	0·61780E − 04	0·27319E − 02	0·74569E − 04	0·78201E − 03	0·10370E − 03
5·0154	3·50	0·10524E − 03	0·20209E + 00	0·94849E − 04	0·42389E − 01	0·90385E − 04	0·11616E − 01	0·93966E − 04	0·34655E − 02	0·11002E − 03	0·10441E − 02	0·14724E − 03
5·3535	3·75	0·15217E − 03	0·22045E + 00	0·13806E − 03	0·47805E − 01	0·13168E − 03	0·13673E − 01	0·13535E − 03	0·42730E − 02	0·15472E − 03	0·13461E − 02	0·20055E − 03
5·6924	4·00	0·20956E − 03	0·23873E + 00	0·19127E − 03	0·53266E − 01	0·18278E − 03	0·15810E − 01	0·18638E − 03	0·51457E − 02	0·20905E − 03	0·16857E − 02	0·26384E − 03
6·0320	4·25	0·27722E − 03	0·25695E + 00	0·25442E − 03	0·58756E − 01	0·24371E − 03	0·18011E − 01	0·24716E − 03	0·60754E − 02	0·27311E − 03	0·20601E − 02	0·33706E − 03
6·3722	4·50	0·35466E − 03	0·27511E + 00	0·32713E − 03	0·64260E − 01	0·31423E − 03	0·20262E − 01	0·31750E − 03	0·70542E − 02	0·34673E − 03	0·24661E − 02	0·41998E − 03
6·7129	4·75	0·44117E − 03	0·29320E + 00	0·40880E − 03	0·69768E − 01	0·39383E − 03	0·22553E − 01	0·39703E − 03	0·80746E − 02	0·42957E − 03	0·29006E − 02	0·51216E − 03
7·0541	5·00	0·53591E − 03	0·31122E + 00	0·49870E − 03	0·75274E − 01	0·48189E − 03	0·24874E − 01	0·48517E − 03	0·91302E − 02	0·52113E − 03	0·33603E − 02	0·61307E − 03

TABLE 3

Continued

(c) Third mode

ω_{n1}^*/ω_1^*	C_1	C_3	C_5	C_7	C_9	C_{11}	C_{13}	C_{15}	C_{17}	C_{19}	C_{21}	C_{23}
1·0028	0·05	− 0·7195E − 09	0·29597E − 10	− 0·3816E − 11	0·52638E − 05	− 0·2751E − 13	0·29468E − 13	0·10667E − 08	0·52572E − 13	− 0·4725E − 13	0·25843E − 12	0·10580E − 13
1·0676	0·25	0·21194E − 11	− 0·1659E − 12	0·50341E − 13	0·63048E − 03	0·11276E − 12	0·71204E − 14	0·31209E − 05	0·19749E − 11	0·40138E − 15	0·18104E − 07	0·61379E − 10
1·2451	0·50	0·17757E − 09	0·43756E − 09	0·62864E − 12	0·44680E − 02	0·55977E − 09	0·24613E − 13	0·82748E − 04	0·26226E − 08	0·71936E − 15	0·17868E − 05	0·22416E − 07
1·4883	0·75	0·39410E − 07	0·55804E − 07	0·66890E − 10	0·12710E − 01	0·50266E − 07	0·84692E − 11	0·48023E − 03	0·12291E − 06	0·59937E − 12	0·21056E − 04	0·53260E − 06
1·7669	1·00	0·10610E − 05	0·10846E − 05	− 0·3454E − 08	0·24782E − 01	0·85584E − 06	− 0·1052E − 09	0·14801E − 02	0·14314E − 05	− 0·2849E − 12	0·10238E − 03	0·40632E − 05
2·0652	1·25	0·96037E − 05	0·79001E − 05	− 0·9340E − 07	0·39543E − 01	0·59219E − 05	− 0·9678E − 08	0·32446E − 02	0·78751E − 05	− 0·1053E − 08	0·30889E − 03	0·16832E − 04
2·3756	1·50	0·45941E − 04	0·32308E − 04	− 0·7580E − 06	0·55987E − 01	0·23737E − 04	− 0·1145E − 06	0·57847E − 02	0·27442E − 04	− 0·1726E − 07	0·69708E − 03	0·48152E − 04
2·6938	1·75	0·14673E − 03	0·91613E − 04	− 0·3373E − 05	0·73416E − 01	0·66796E − 04	− 0·6486E − 06	0·90140E − 02	0·70832E − 04	− 0·1219E − 06	0·13005E − 02	0·10809E − 03
3·0174	2·00	0·35750E − 03	0·20326E − 03	− 0·1035E − 04	0·91387E − 01	0·14780E − 03	− 0·2372E − 05	0·12806E − 01	0·14851E − 03	− 0·5270E − 06	0·21275E − 02	0·20509E − 03
3·3450	2·25	0·72077E − 03	0·37998E − 03	− 0·2475E − 04	0·10963E + 00	0·27608E − 03	− 0·6479E − 05	0·17033E − 01	0·26812E − 03	− 0·1642E − 05	0·31667E − 02	0·34463E − 03
3·6757	2·50	0·12672E − 02	0·62776E − 03	− 0·4960E − 04	0·12798E + 00	0·45606E − 03	− 0·1441E − 04	0·21581E − 01	0·43339E − 03	− 0·4057E − 05	0·43949E − 02	0·52880E − 03
4·0086	2·75	0·20123E − 02	0·94634E − 03	− 0·8730E − 04	0·14634E + 00	0·68755E − 03	− 0·2756E − 04	0·26359E − 01	0·64430E − 03	− 0·8450E − 05	0·57836E − 02	0·75677E − 03
4·3435	3·00	0·29574E − 02	0·13309E − 02	− 0·1394E − 03	0·16466E + 00	0·96704E − 03	− 0·4705E − 04	0·31294E − 01	0·89802E − 03	− 0·1547E − 04	0·73039E − 02	0·10256E − 02
4·6798	3·25	0·40932E − 02	0·17742E − 02	− 0·2064E − 03	0·18291E + 00	0·12891E − 02	− 0·7358E − 04	0·36333E − 01	0·11900E − 02	− 0·2563E − 04	0·89289E − 02	0·13309E − 02
5·0174	3·50	0·54035E − 02	0·22677E − 02	− 0·2880E − 03	0·20107E + 00	0·16475E − 02	− 0·1074E − 03	0·41436E − 01	0·15151E − 02	− 0·3926E − 04	0·10635E − 01	0·16678E − 02
5·3561	3·75	0·68684E − 02	0·28031E − 02	− 0·3835E − 03	0·21913E + 00	0·20361E − 02	− 0·1485E − 03	0·46574E − 01	0·18678E − 02	− 0·5650E − 04	0·12402E − 01	0·20315E − 02
5·6957	4·00	0·84667E − 02	0·33724E − 02	− 0·4915E − 03	0·23710E + 00	0·24491E − 02	− 0·1965E − 03	0·51727E − 01	0·22432E − 02	− 0·7733E − 04	0·14215E − 01	0·24172E − 02
6·0360	4·25	0·10178E − 01	0·39688E − 02	− 0·6107E − 03	0·25497E + 00	0·28815E − 02	− 0·2507E − 03	0·56881E − 01	0·26367E − 02	− 0·1016E − 03	0·16060E − 01	0·28208E − 02
6·3770	4·50	0·11983E − 01	0·45864E − 02	− 0·7396E − 03	0·27276E + 00	0·33290E − 02	− 0·3106E − 03	0·62025E − 01	0·30446E − 02	− 0·1290E − 03	0·17928E − 01	0·32386E − 02
6·7186	4·75	0·13865E − 01	0·52203E − 02	− 0·8768E − 03	0·29046E + 00	0·37880E − 02	− 0·3755E − 05	0·67154E − 01	0·34634E − 02	− 0·1594E − 03	0·19809E − 01	0·36675E − 02
7·0607	5·00	0·15810E − 01	0·58664E − 02	− 0·1021E − 02	0·30809E + 00	0·42556E − 02	− 0·4447E − 03	0·72262E − 01	0·38906E − 02	− 0·1923E − 03	0·21699E − 01	0·41049E − 02

TABLE 3

Continued

(d) Fourth mode

ω_{nl}^*/ω_l^*	C_2	C_4	C_6	C_8	C_{10}	C_{12}	C_{14}	C_{16}	C_{18}	C_{20}	C_{22}	C_{24}
1·0028	0·05	−0·39751E−10	−0·2898E−11	0·58726E−12	−0·1327E−13	0·52638E−05	0·25104E−13	0·13458E−13	−0·96515E−14	0·10666E−08	0·17641E−12	0·98798E−14
1·0676	0·25	0·49818E−10	0·27462E−09	0·31778E−13	0·23795E−12	0·63048E−03	0·75661E−09	−0·2032E−14	0·21744E−14	0·31207E−05	0·12388E−07	−0·5182E−14
1·2451	0·50	0·15529E−06	0·23355E−06	0·11944E−12	0·23293E−08	0·44680E−02	0·26110E−06	0·20713E−12	0·74323E−10	0·82686E−04	0·12079E−05	0·93645E−12
1·4883	0·75	0·86570E−05	0·64803E−05	0·13894E−09	0·21997E−06	0·12709E−01	0·57106E−05	0·15324E−09	0·14302E−07	0·47876E−03	0·14032E−04	0·36602E−09
1·7669	1·00	0·96536E−04	0·45477E−04	0·90275E−08	0·32254E−05	0·24773E−01	0·38886E−04	0·80701E−08	0·32875E−06	0·14690E−02	0·67256E−04	0·13325E−07
2·0653	1·25	0·47327E−03	0·15785E−03	0·13413E−06	0·18440E−04	0·39500E−01	0·14029E−03	0·10827E−06	0·25449E−05	0·31990E−02	0·19966E−03	0·14277E−06
2·3758	1·50	0·14426E−02	0·36510E−03	0·85542E−06	0·61597E−04	0·55859E−01	0·34486E−03	0·65559E−06	0·10511E−04	0·56568E−02	0·44173E−03	0·75035E−06
2·6943	1·75	0·32655E−02	0·65671E−03	0·32355E−05	0·14766E−03	0·73126E−01	0·66328E−03	0·24136E−05	0·29356E−04	0·87338E−02	0·80459E−03	0·25200E−05
3·0185	2·00	0·60704E−02	0·10031E−02	0·87061E−05	0·28500E−03	0·90847E−01	0·10835E−02	0·64044E−05	0·63414E−04	0·12289E−01	0·12809E−02	0·62889E−05
3·3468	2·25	0·98498E−02	0·13724E−02	0·18586E−04	0·47444E−03	0·10875E+00	0·15823E−02	0·13579E−04	0·11491E−03	0·16189E−01	0·18524E−02	0·12787E−04
3·6784	2·50	0·14504E−01	0·17402E−02	0·33718E−04	0·71144E−03	0·12668E+00	0·21351E−02	0·24568E−04	0·18391E−03	0·20322E−01	0·24969E−02	0·22467E−04
4·0124	2·75	0·19891E−01	0·20914E−02	0·54374E−04	0·98877E−03	0·14455E+00	0·27213E−02	0·39601E−04	0·26893E−03	0·24605E−01	0·31939E−02	0·35471E−04
4·3485	3·00	0·25860E−01	0·24186E−02	0·80352E−04	0·12985E−02	0·16232E+00	0·33257E−02	0·58576E−04	0·36772E−03	0·28977E−01	0·39264E−02	0·51690E−04
4·6862	3·25	0·32274E−01	0·27197E−02	0·11115E−03	0·16334E−02	0·17996E+00	0·39379E−02	0·81158E−04	0·47780E−03	0·33396E−01	0·46812E−02	0·70849E−04
5·0253	3·50	0·39016E−01	0·29956E−02	0·14611E−03	0·19870E−02	0·19749E+00	0·45510E−02	0·10690E−03	0·59682E−03	0·37833E−01	0·54488E−02	0·92585E−04
5·3655	3·75	0·45993E−01	0·32488E−02	0·18454E−03	0·23541E−02	0·21490E+00	0·51611E−02	0·13531E−03	0·72271E−03	0·42269E−01	0·62226E−02	0·11651E−03
5·7066	4·00	0·53130E−01	0·34825E−02	0·22580E−03	0·27307E−02	0·23219E+00	0·57659E−02	0·16591E−03	0·85373E−03	0·46693E−01	0·69980E−02	0·14225E−03
6·0485	4·25	0·60408E−01	0·37126E−02	0·24522E−03	0·32030E−02	0·24932E+00	0·62834E−02	0·20277E−03	0·84422E−03	0·51064E−01	0·78120E−02	0·72606E−04
6·3912	4·50	0·67677E−01	0·39032E−02	0·31453E−03	0·35006E−02	0·26647E+00	0·69557E−02	0·23205E−03	0·11259E−02	0·55479E−01	0·85429E−02	0·19782E−03
6·7344	4·75	0·75013E−01	0·40955E−02	0·36108E−03	0·38897E−02	0·28348E+00	0·75404E−02	0·26690E−03	0·12650E−02	0·59834E−01	0·93093E−02	0·22711E−03
7·081	5·00	0·82358E−01	0·42788E−02	0·40861E−03	0·42797E−02	0·30041E+00	0·81185E−02	0·30255E−03	0·14053E−02	0·64162E−01	0·10071E−01	0·25710E−03

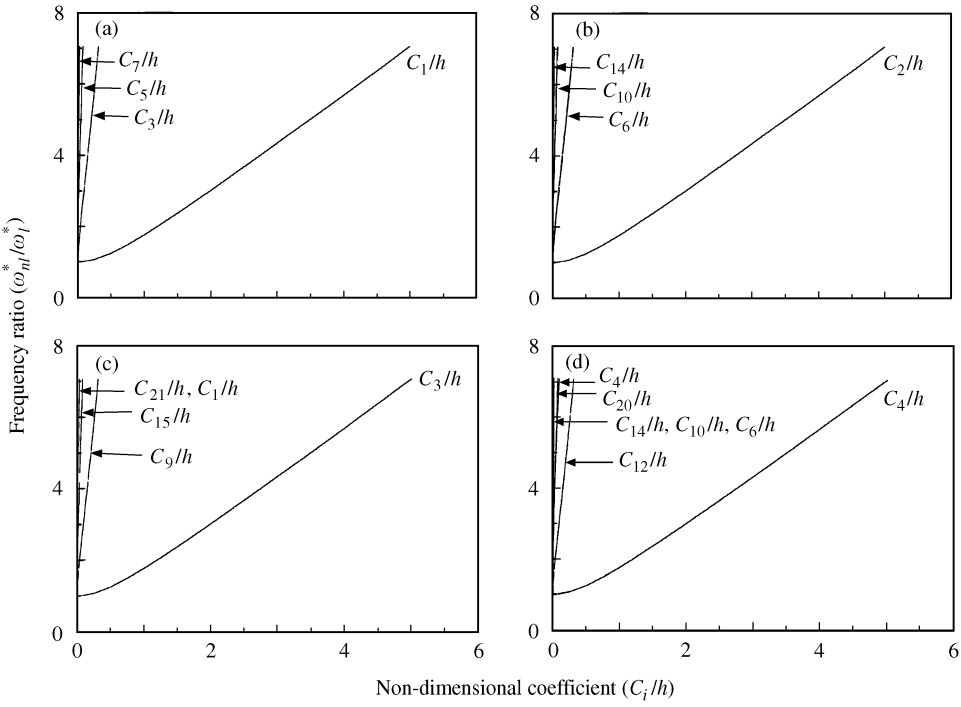

Figure 3. Basic function contribution coefficients to (a) first non-linear mode shape; (b) second non-linear mode shape and (c) third non-linear mode shape and (d) fourth non-linear mode shape, for $\beta = 0{\cdot}05$.

corresponding to c_4 varying from 0·05 to 5 for the fourth mode and their associated non-linear frequency ratios $(\omega^*_{nl}/\omega^*_l)_4$ are presented in Table 3(d). It can be seen from Table 3(a–d) that the rate of increase in non-linear fundamental frequency with increasing displacement is very low at small amplitudes, for a given shell thickness. This can lead to the conclusion that the practical use of the linear frequencies for such amplitudes can be of acceptable accuracy, although it must limit the expected frequency estimate accuracy to a reasonable range.

In Figure 3(a–d), the basic function coefficients, corresponding to an infinite shell having 0·05 as thickness to radius ratio, are plotted versus the non-linear frequency ratio $(\omega^*_{nl}/\omega^*_l)_i$ (ω^*_l is the corresponding linear frequency parameter given in references [41, 42]), for the first, second, third and fourth mode shapes. It can be observed that near the linear frequency of a given mode only the corresponding basic function has a significant contribution. At large displacements amplitudes, the higher mode contribution coefficients and resonance frequencies increase (see Table 2 in which ω^*_{nl} alone are presented for the first four modes), but the non-linear frequency ratio $(\omega^*_{nl}/\omega^*_l)_i$ dependence on c_i is almost identical for all values of i considered here (see also Table 3(a–d)).

The normalized first four mode shapes are plotted in Figure 4(a–d) for the values of the vibration normalized amplitude W^*/W^*_{max} and ω^*_{nl} given in Table 4(a–d). It can be seen that all are amplitude dependent and the non-linearity effect is qualitatively the same for the first four non-linear mode shapes. This last characteristic appears clearly in Figure 4, by looking at the collapse between the linear curve (i.e., curve (1)) and the most external non-linear curve (i.e., (5)). This fact is confirmed quantitatively by no change in the frequency parameter ratio $(\omega^*_{nl}/\omega^*_l)_i$ with increasing mode order (see Table 3).

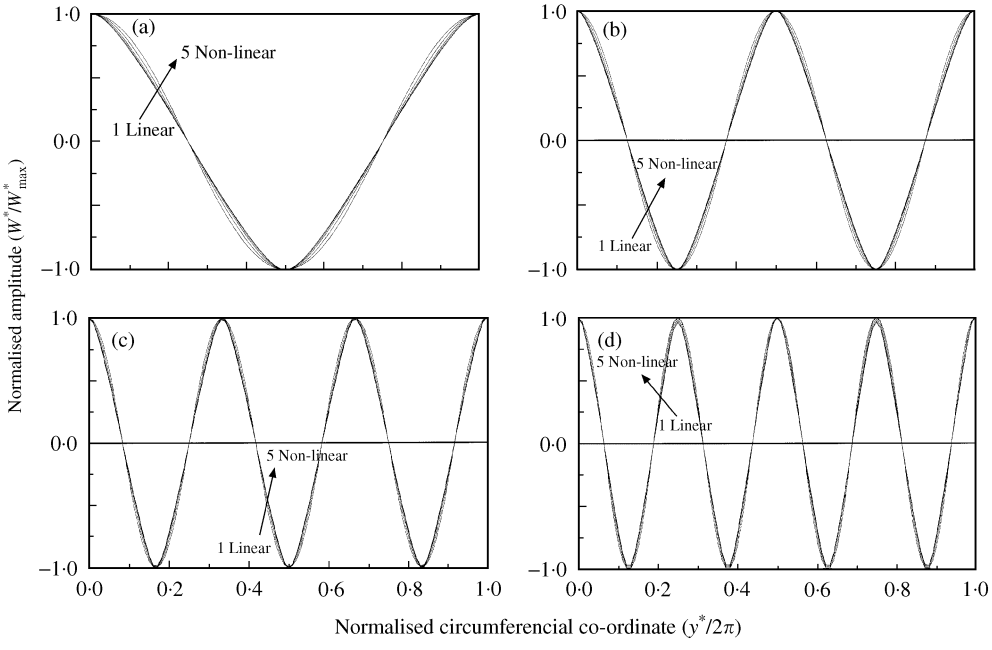

Figure 4. Theoretical non-linear first mode shapes of a circular cylindrical shell of infinite length with $\beta = 0{\cdot}5$ for (a) curves numbered 1–5 see Table 4(a); (b) curves numbered 1–5 see Table 4(b); (c) curves numbered 1–5 see Table 4(c); (d) curves numbered 1–5 see Table 4(d).

3.5. EFFECT OF GEOMETRICAL NON-LINEARITY ON THE NATURAL FREQUENCIES OF INFINITE SHELLS HAVING VARIOUS THICKNESS TO RADIUS RATIO β

To illustrate the effect of geometrical non-linearity, numerical results have been presented for the first non-linear mode. Low values of $\beta = h/R$ represent the behaviour of very thin infinite shells, while large values of β reflect the behaviour of moderate thin shells. Representative curves, depicting these behaviours, are given in Figure 5. It can be seen that no detectable non-linearity is observed for values of the ratio β less than 0·001 and for a given value of c_1. However, the non-linear frequency parameter depends strongly on the parameter (h/R). It may be surprising to find that one compares the non-linear behaviour of shells of the same radius R, the non-linear frequency increases with β, which means that it increases with the thickness h. On one hand, this fact is mathematically due to the presence of a coefficient β^2, which is very small for small values of β, in the expression of the non-linear term $\mathbf{b}^*_{ijkl}$ (see equation (15)). On the other hand, it should not be forgotten that as $c_1 = w_1/h$, when a comparison is made for the same value of c_1, for example $c_1 = 2{\cdot}5$ corresponding to the horizontal line of Figure 5, the actual physical amplitude of vibration $w_1 = c_1 h = 2{\cdot}5h$, is also increasing with h for shells assumed to have the same radius R. So, the comparison is made between shells having the same radius R, but increasing values of the physical amplitude of vibration displacement and hence increasing stretching effect, which explains the increase in the non-linear effect, with increasing β.

3.6. FORMS OF THE CIRCUMFERENTIAL NODAL PATTERNS ASSOCIATED WITH THE FIRST FIVE NON-LINEAR MODE SHAPES OF INFINITE SHELLS COMPARISON WITH LINEAR RESULTS

To determine the non-linear modes and show the effect of non-linearity on the natural mode shapes of an infinite cylinder, the undeformed circumference of the cylinder and the

TABLE 4

Maximum normalized amplitude and frequency parameters corresponding to the first four non-linear mode shapes and curvatures plotted in Figure 4(a–d)

Curves	W^*_{max}	ω^*_{nl}
(a) First mode		
1	0·05000526	0·01447428
2	1·29313848	0·02980875
3	2·65601182	0·05304729
4	4·03868611	0·07726872
5	5·42829728	0·10180685
(b) Second mode		
1	0·05000527	0·05789714
2	1·29313827	0·11923500
3	2·65598944	0·21218956
4	4·03845498	0·30908327
5	5·42699929	0·40726778
(c) Third mode		
1	0·05000526	0·13026856
2	1·29314441	0·26827911
3	2·65719985	0·47748176
4	4·04310406	0·69577887
5	5·43424725	0·91720896
(d) Fourth mode		
1	0·05000526	0·23158855
2	1·29369141	0·47695899
3	2·66885208	0·84948480
4	4·07130428	1·23909784
5	5·47605175	1·63462264

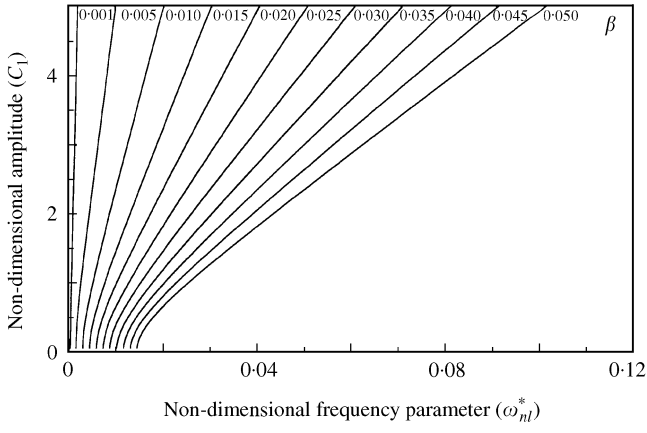

Figure 5. The effect of frequency upon large vibration amplitude for various thickness to radius ratios of a circular cylindrical shell of infinite length at first mode.

form of the linear and non-linear mode shapes are plotted in Figures 6–10. These figures correspond to the first five modes when the non-dimensional transverse vibration parameter C_i/h varies from 0·05 to 10, and for values of the thickness to radius ratios equal

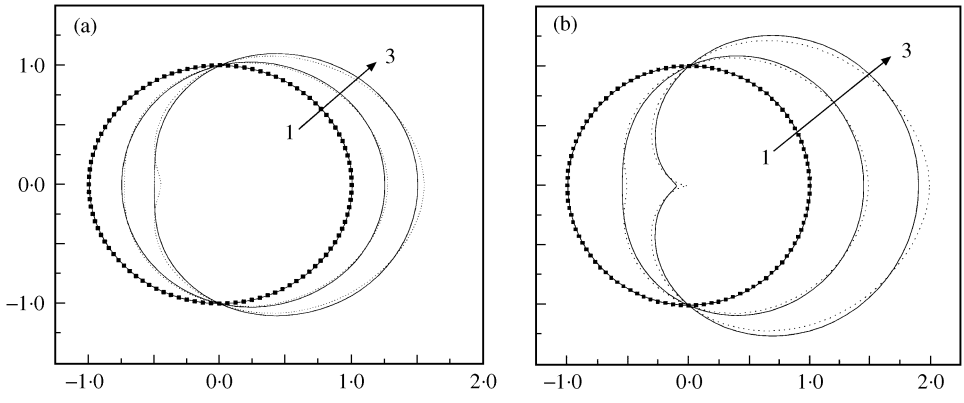

Figure 6. Comparison of non-linear (dashed lines) and linear (thin solid lines) circumferential nodal patterns of the first mode shapes for thickness to radius ratios (a) $\beta = 0{\cdot}05$ and (b) $\beta = 0{\cdot}09$. Non-dimensional vibration amplitudes C_1/h and non-linear frequency parameters ω^*_{n1} are equal to: (a) curve 1, (0·05; 0·01447); curve 2, (5; 0·10181); curve 3, (10; 0·20091); (b) curve 1, (0·05; 0·02605); curve (2), (5; 0·18325); curve 3, (10; 0·36163). Undeformed cylinder. —■—.

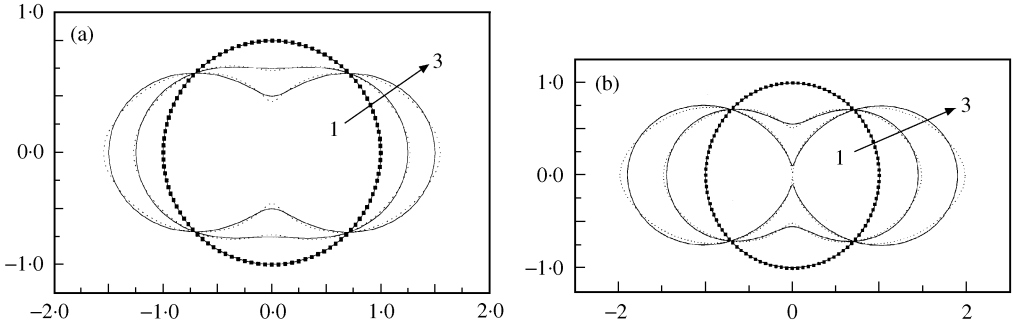

Figure 7. Comparison of non-linear (dashed lines) and linear (thin solid lines) circumferential nodal patterns of the second mode shapes for thickness to radius ratios (a) $\beta = 0{\cdot}05$ and (b) 0·09. Non-dimensional vibration amplitudes C_2/h and non-linear frequency parameters ω^*_{n1} are equal to: (a) curve 1, (0·05; 0·057897); curve 2, (5; 0·40541); curve 3, (10; 0·80410); (b) curve 1, (0·05; 0·1042); curve 2, (5; 0·7331); curve 3, (10; 1·4474). Undeformed cylinder, —■—.

to 0·05 (see Figures 6(a)–10(a)) and 0·09 (see Figures 6(b)–10(b)). In each figure, the non-linear frequency parameter and the corresponding vibration displacement amplitudes are given. The shape of the undeformed cylinder is plotted in small squares, the linear modes are plotted with thin solid lines and the non-linear modes are plotted with dashed lines. It is observed that all modes are deformed either positively (dilation) or negatively (compression) under the non-linearity effect. These deformations increase with increasing vibration amplitude and thickness to radius ratio. Of course, the vibration frequency also increases when the deformation increases. It can also be seen that the deformations due to non-linearity are important particularly at point $y^* = 0$ and π for the first four modes. For the fifth non-linear mode these deformations are equal and homogeneously distributed. In these figures, it can be seen that the symmetrical form of the even linear mode shapes is conserved for the non-linear modes shapes. The same characteristic is clear for the asymmetrical form of the odd mode shapes. Therefore, to complete the study of the dynamical behaviour and evaluate quantitatively these deformations, an analysis of the

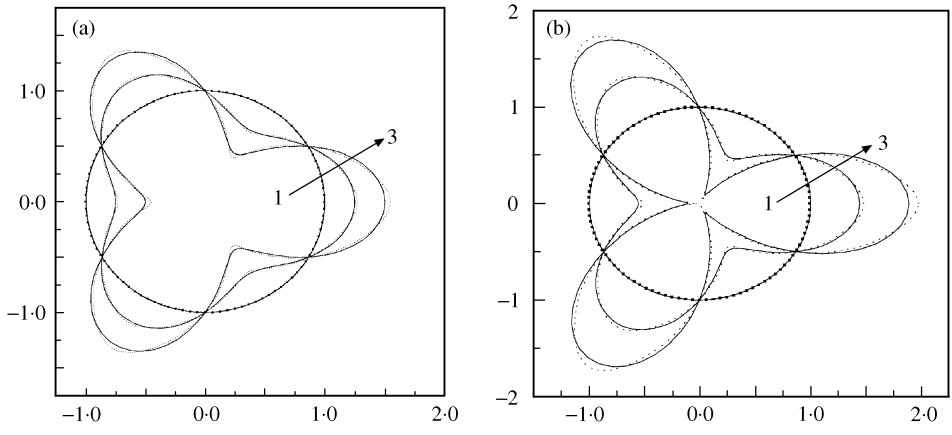

Figure 8. Comparison of non-linear (dashed lines) and linear (thin solid lines) circumferential nodal patterns of the third mode shapes for thickness to radius ratios (a) $\beta = 0{\cdot}05$ and (b) $\beta = 0{\cdot}09$. Non-dimensional vibration amplitudes C_3/h and non-linear frequency parameters ω_{nl}^* are equal to: (a) curve 1, (0·05; 0·1303); curve 2, (5; 0·9172); curve 3, (10; 1·8128); (b) curve 1; (0·05; 0·2345); curve 2, (5; 1·6510), curve 3; (10; 3·2630). undeformed cylinder, —■—.

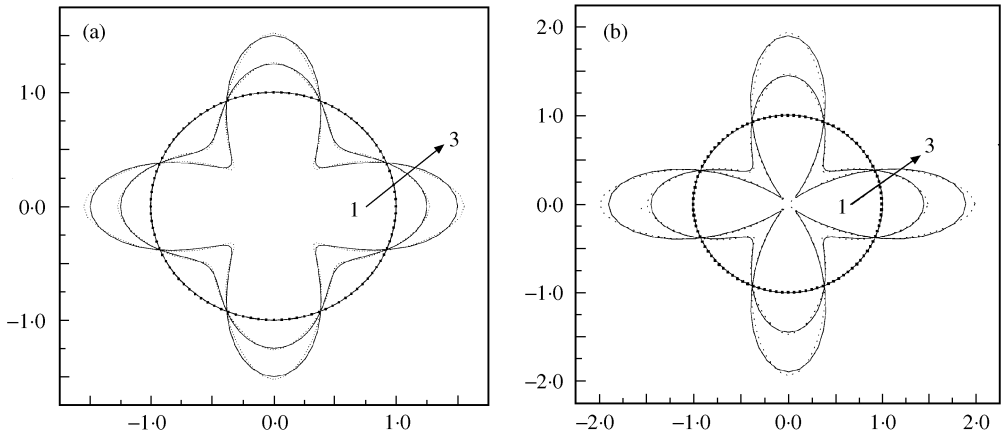

Figure 9. Comparison of non-linear (dashed lines) and linear (thin solid lines) circumferential nodal patterns of the fourth mode shapes for thickness to radius (a) $\beta = 0{\cdot}05$ and (b) 0·09. Non-dimensional vibration amplitudes C_4/h and non-linear frequency parameters ω_{nl}^* are equal to: (a) curve 1, (0·05; 0·2316), curve 2, (5; 1·6346); curve 3, (10; 3·2342); (b) curve 1, (0·05; 0·4166); curve 2, (5; 2·9423); curve 3, (10; 5·8215). undeformed cylinder, —■—.

corresponding bending stress distribution is necessary to show how much the non-linear effect influences the dynamic behaviour of the structure.

3.7. NON-LINEAR EFFECT ON THE BENDING STRESS DISTRIBUTION. COMPARISON WITH LINEAR RESULTS

The bending stress distributions along the external circumferential co-ordinate corresponding to the first four non-linear mode shapes are plotted in Figures 11–14 for various vibration displacement amplitudes c_i varying from 0·05 up to 3 times the thickness

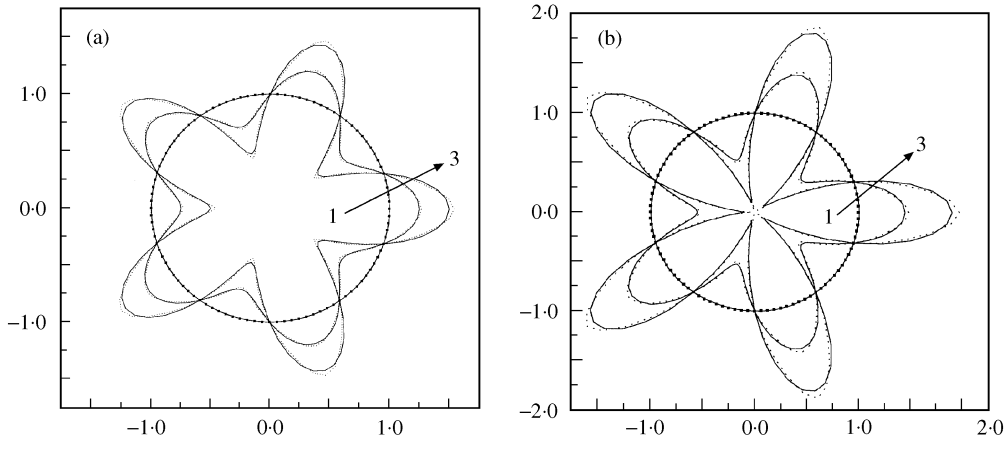

Figure 10. Comparison of non-linear (dashed lines) and linear (thin solid lines) circumferential nodal patterns of the fifth mode shapes for thickness to radius (a) $\beta = 0{\cdot}05$ and (b) $\beta = 0{\cdot}09$. Non-dimensional vibration amplitudes C_5/h and non-linear frequency parameters ω_{n1}^* are equal to: (a) curve 1, (0·05; 0·2316); curve 2, (5; 1·6346); curve 3, (10; 3·2342); (b) curve 1, (0·05; 0·4166); curve 2, (5; 2·9423); curve 3, (10; 5·8215).

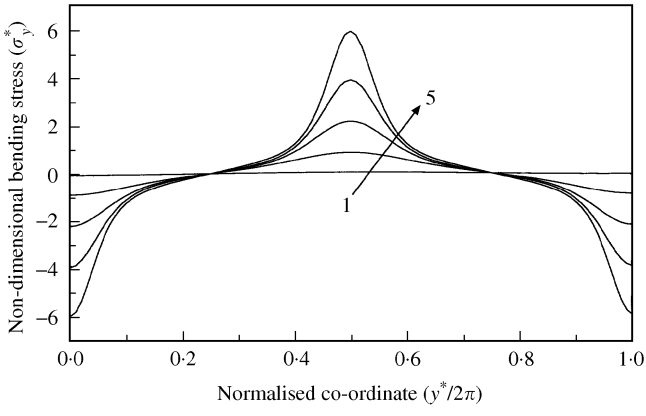

Figure 11. Non-dimensional bending stress distribution along the shell circumference for the first non-linear mode for vibration amplitudes C_1/h, $\beta = 0{\cdot}05$ and non-linear frequency parameters ω_{n1}^* equal to: curve 1, (0·05; 0·014474); curve 2, (0·75; 0·021482); curve 3, (1·5; 0·034288); curve 4, (2·25; 0·048278) and curve 5, (3; 0·062677).

(with i = first mode to fourth mode). It can be seen that the stresses increase with increasing vibration amplitude and the mode order. It is also observed that all these stress distributions admit a maximum and a minimum and regions of stress concentration around them. So, for the first mode the maximal stress is found at circumference point $y^*/2\pi = 0{\cdot}5$, for the second mode it is at $y^*/2\pi = 0{\cdot}25$ and 0·75, for the third mode it is at $y^*/2\pi = 0{\cdot}167$, 0·5 and 0·833 and for the fourth mode it is at $y^*/2\pi = 0{\cdot}125$, 0·5, 0·625 and 0·75. The repartition of these maximums conforms to the mode shape presented above (see Figures 6–9).

A comparison of the bending stress obtained in the linear case (by putting $\mathbf{b}_{ijkl}^* = 0$ in the present model) with that obtained when the non-linear effect is introduced is presented in Figures 15–18 for the first four mode shapes. It can be seen that all curves show the

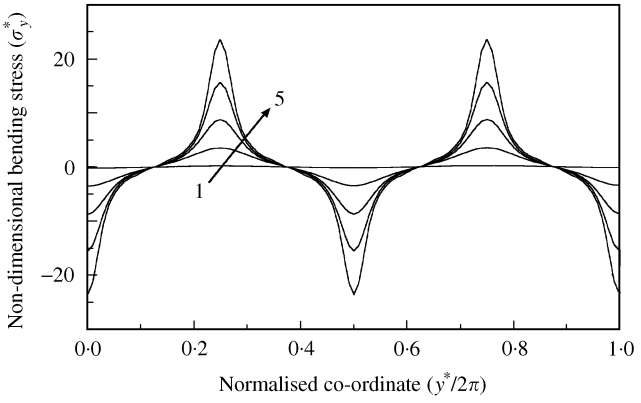

Figure 12. Non-dimensional bending stress distribution along the shell circumference for the second non-linear mode for vibration amplitudes C_2/h, $\beta = 0{\cdot}05$ and non-linear frequency parameters ω_{n1}^* equal to: curve 1, (0·05; 0·057897); curve 2, (0·75; 0·085927); curve 3, (1·5; 1·371521); curve 4, (2·25; 1·931119) and curve 5, (3; 2·507089).

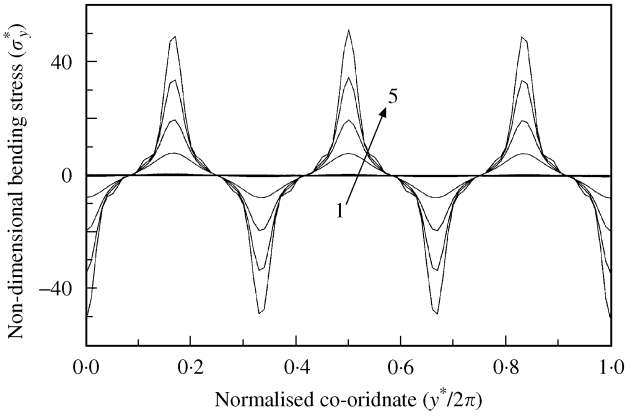

Figure 13. Non-dimensional bending stress distribution along the shell circumference for the third non-linear mode for vibration amplitudes C_3/h, $\beta = 0{\cdot}05$ and non-linear frequency parameters ω_{n1}^* equal to: curve 1, (0·05; 0·130269); curve 2, (0·75; 0·193338); curve 3, (1·5; 0·308594); curve 4, (2·25; 0·434532) and curve 5, (3; 0·564232).

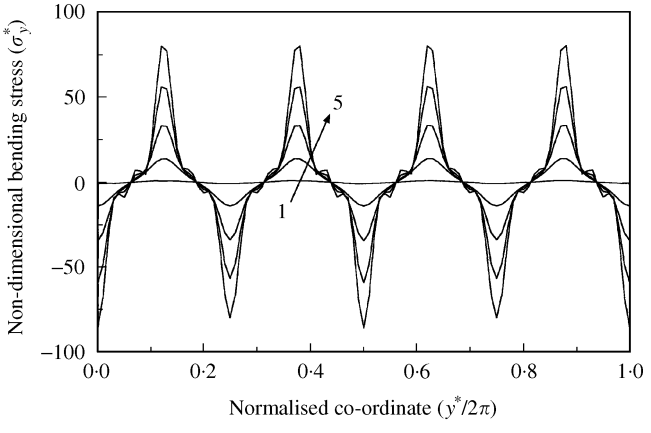

Figure 14. Non-dimensional bending stress distribution along the shell circumference for the fourth non-linear mode for vibration amplitudes C_4/h, $\beta = 0{\cdot}05$ and non-linear frequency parameters ω_{n1}^* equal to: curve 1, (0·05; 0·231589); curve 2, (0·75; 0·343711); curve 3, (1·5; 0·548669); curve 4, (2·25; 0·772919) and curve 5, (3; 1·004242).

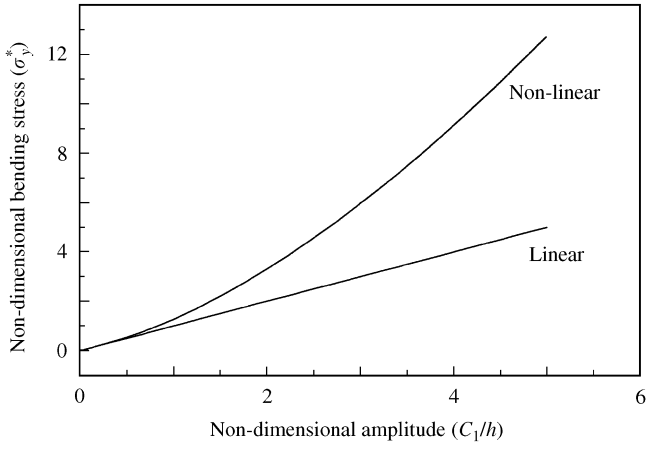

Figure 15. Effect of large vibration amplitudes on the non-dimensional bending stress corresponding to the first mode at shell circumference points $y^*/2\pi = 0{\cdot}5$, with $\beta = 0{\cdot}05$.

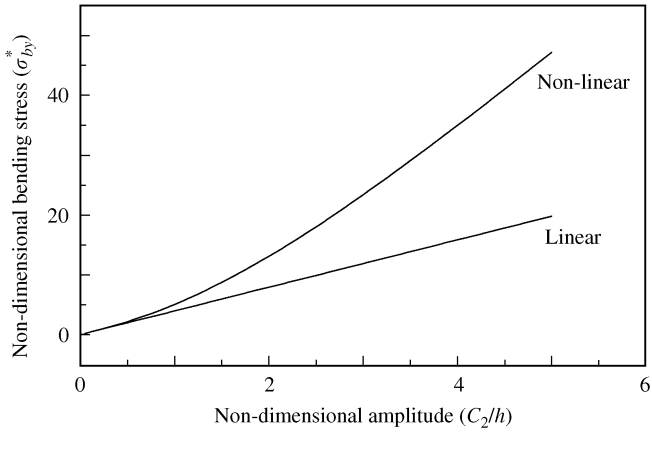

Figure 16. Effect of large vibration amplitudes on the non-dimensional bending stress corresponding to the second mode at shell circumference point $y^*/2\pi = 0{\cdot}25$, with $\beta = 0{\cdot}05$.

amplitude dependence of the stress distribution, and exhibit clearly a high increase of the bending stress, compared with the rate of increase expected in the linear theory.

3.8. NATURAL FREQUENCIES OF THE HIGHER MODES ASSOCIATED WITH THE LONGITUDINAL FUNDAMENTAL MODE OF FINITE CIRCULAR CYLINDRICAL SHELLS. APPROXIMATE SOLUTION

Using the analytical approach formulated above for the infinite length shell, numerical solutions of the set of non-linear algebraic equations (26) are obtained at small vibration amplitudes. These results are compared with those obtained by analytical methods of several authors for finite cylindrical shells vibrating at small vibration amplitudes (linear case) [27–29]. Table 5 reproduces these results together with the corresponding theoretical values computed in the present analysis. The authors of these works have used a laborious

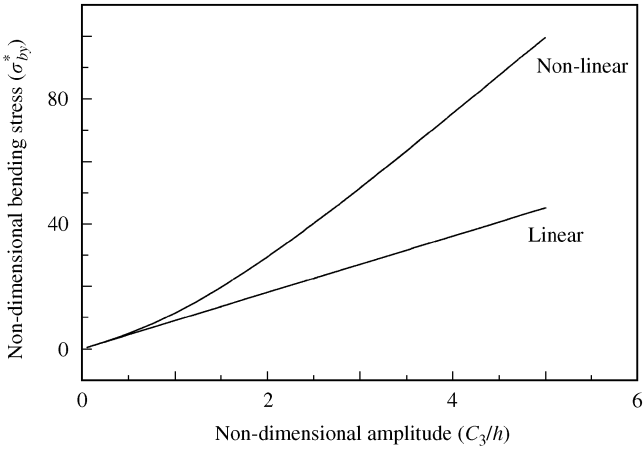

Figure 17. Effect of large vibration amplitudes on the non-dimensional bending stress corresponding to the third mode at shell circumference point $y^*/2\pi = 0{\cdot}5$, with $\beta = 0{\cdot}05$.

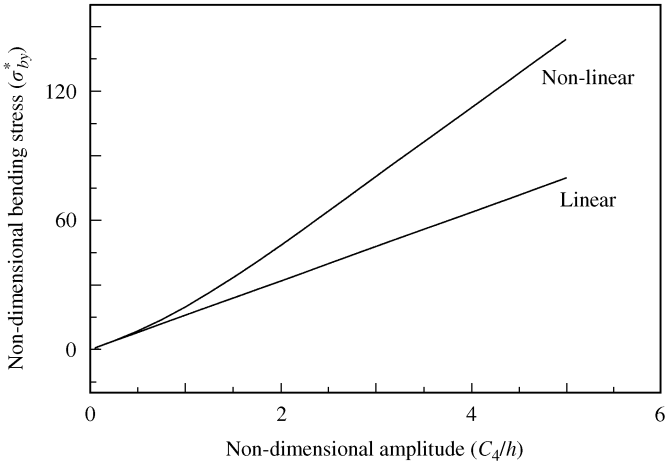

Figure 18. Effect of large vibration amplitude on the non-dimensional bending stress corresponding to the fourth mode at shell circumference point $y^*/2\pi = 0{\cdot}125$, with $\beta = 0{\cdot}05$.

formulation including the longitudinal, circumferential (tangential) and transverse displacement U, V and W respectively. This fact complicated the formulation and consequently the solution of equations. The same results have been obtained via the present model for small vibration amplitudes quite easily.

To provide additional comparison of numerical solutions of equations (26), a set of experimental studies, reported in references [27–29], was considered. Table 6 regroups these results for relatively long, very thin and moderate thin shells. The geometrical and physical characteristics are given in each case. It can be seen, from Tables 5 and 6 that, in general, the natural frequencies obtained from the present analysis agree quite well with results from other analytical methods and experiment data, in particular, for higher values of circumferential mode number n and small axial mode number m. The accuracy of the present approximation increases with the length to radius ratio. It can be noticed that

TABLE 5

Comparison of frequencies (Hz) obtained for small vibration amplitude from solution of the set of non-linear algebraic equations (26)*, using the multi-mode approach, of a circular cylindrical shell of infinite length, with linear theoretical results of finite circular cylindrical shells obtained by different analytical methods* ($\beta = h/R$; $\xi = L/R$)

		Circumferencial mode no. (n)				
Characteristics of shell	References	2	3	4	5	6
$\beta = 0{\cdot}0114$, $\xi = 4{\cdot}11$	Yang [28]	–	–	184	253	355
$\rho = 8020\,\mathrm{kg/m^3}$, $\nu = 0{\cdot}30$	Present work	–	–	156	244	352
$E = 1{\cdot}951 \times 10^{11}\,\mathrm{N/m^2}$						
$\beta = 0{\cdot}0075$, $\xi = 5{\cdot}2$	Coupry [27]	–	–	165	231	342
$\rho = 7800\,\mathrm{kg/m^3}$, $\nu = 0{\cdot}3$	Present work	–	–	146	229	329
$E = 2 \times 10^{11}\,\mathrm{N/m^2}$						
$\beta = 0{\cdot}00675$, $\xi = 7{\cdot}35$	Coupry [27]	–	–	68	104	–
$\rho = 7800\,\mathrm{kg/m^3}$, $\nu = 0{\cdot}3$	Present work	–	–	66	103	–
$E = 2 \times 10^{11}\,\mathrm{N/m^2}$						
$\beta = 0{\cdot}0525$, $\xi = 8{\cdot}0868$	Yang [28]	1485	2364	4147	6504	9396
$\rho = 7840\,\mathrm{kg/m^3}$, $\nu = 0{\cdot}29$	Exact method of Smith and Haft [28]	1429	2336	4142	6500	9400
$E = 2{\cdot}041 \times 10^{11}\,\mathrm{N/m^2}$	Approximate method of Smith and Haft [28]	1575	2784	4192	6565	9453
	Method of Arnold and Warburton [28]	1147	2092	3892	6249	9134
	Present work	1053	2370	4213	6582	9478

among 15 natural frequencies measured, 11 are better predicted by the present approximation with no discrepancy larger than 10%.

Consequently, it can be concluded, in the light of these comparisons, that the model presented here, can be used for describing the dynamic behaviour of finite cylinders having a length L larger than about six times the radius. This approach is valuable for the fundamental longitudinal mode ($m = 1$) and high circumferential number mode ($n > 3$) and has the advantage of simplicity compared with previous works.

4. CONCLUSIONS

Analytical and numerical results have been presented in this paper for the non-linear free vibration of cylindrical shells. The objectives were (1) to develop a semi-analytical model, based on Hamilton's principle and spectral analysis, permitting easy calculation of the non-linear transverse mode shapes and their corresponding frequencies for cylindrical shells of infinite length: (2) to validate the model via comparison with previously published results, and (3) to give supplementary new results, especially the frequencies, bending stress distributions and the associated non-linear mode shapes taking into account the contribution of the higher modes. It has been shown that the forms of the mode shapes, at large vibration amplitudes, exhibit clearly a deformation for moderate thin shells if non-linear effects due to large vibration amplitudes are taken into account. It is interesting to note that the non-linearity can affect significantly the bending stresses in such types of

TABLE 6

Comparison of frequencies (Hz) obtained, for small vibration amplitude, from solution of the set of non-linear algebraic equations (26), *using the multi-mode approach, of a circular cylindrical shell of infinite length, with experimental results for a finite circular cylindrical shell obtained by several authors in the linear case* ($\beta = h/R$; $\xi = L/R$)

Characteristics of shell	$\beta = 0{\cdot}0114$, $\xi = 4{\cdot}11$ $\rho = 8020\,\mathrm{kg/m^3}$, $\nu = 0{\cdot}30$ $E = 1{\cdot}95 \times 10^{11}\,\mathrm{N/m^2}$			$\beta = 0{\cdot}0075$, $\xi = 5{\cdot}2$ $\rho = 7800\,\mathrm{kg/m^3}$, $\nu = 0{\cdot}3$ $E = 2 \times 10^{11}\,\mathrm{N/m^2}$			$\beta = 0.00675$, $\xi = 7.35$ $\rho = 7800\,\mathrm{kg/m^3}$, $\nu = 0{\cdot}3$ $E = 2 \times 10^{11}\,\mathrm{N/m^2}$			$\beta = 0{\cdot}0525$, $\xi = 8{\cdot}10$ $\rho = 7840\,\mathrm{kg/m^3}$, $\nu = 0{\cdot}29$ $E = 2.04 \times 10^{11}\,\mathrm{N/m^2}$		
Mode no. (n)	[28]	ε^* (%)	P.W	[27]	ε (%)	P.W	[27]	ε (%)	P.W	[29]	ε (%)	P.W
3	214	–	88	–	–	–	60	–	37	2150	9.28	2370
4	199	27.56	156	174	19.18	146	68	3.03	66	3970	5.77	4213
5	256	4.92	244	240	4.80	229	106	2.90	103	6320	3.98	6582
6	324	7.95	352	329	0.00	329	–	–	148	9230	2.62	9478
7	–	–	–	447	0.22	448	–	–	–	–	–	–

P.W: present work and $\varepsilon^* = ([..] - \mathrm{P.W})/\mathrm{P.W}$.

structures and will certainly modify the predicted fatigue life. It can be concluded also, in the light of the discussion concerning the finite simply supported cylindrical shell results presented in section 3.8, that the semi-analytical model presented here, can be considered as a good approximation in many engineering applications in which shells vibrate non-linearly at small amplitudes with higher values of circumferential mode number n ($n > 3$) associated to the fundamental longitudinal mode shape ($m = 1$). It is noticable that this approach is easily exploited and simplifies considerably the mathematical analysis describing the dynamic behaviour of finite cylindrical shells. On the other hand, the analysis presented in this paper is independent of the axial wavelength and can be used without imposing any restriction on the shell boundary conditions. It represents the asymptotic results for a given n and $\beta = h/R$ when $L/R \to \infty$ but does not represent a general solution of the dynamic behaviour of finite shells. Study of this subject will be completed by development of a non-linear vibration general model of finite cylindrical shells, in a later work (Part III) of this series of papers.

REFERENCES

1. C. Mei and C. B. Prasad 1987 *Journal of Sound and Vibration* **117**, 173–186. Effects of non-linear damping on random response of beams to acoustic loading.
2. W. Han and M. Petyt 1997 *Computer and Structures* **63**, 295–308. Geometrical non-linear vibration analysis of thin, rectangular plates using the hierarchical finite element method—I: the fundamental mode of isotropic plates.
3. M. P. Nemeth, R. D. Young, T. J. Collins and J. H. Starnes 1998 *Proceeding of the 39th AIAA/ASME/ASCE/AHS/ASC Structures, Structural Dynamics, and Material Conference*. Non-linear analysis of the space shuttle super-lightweight LO_2 tank: Part II—behaviour under 3g end-of-flight loads.
4. M. Ganapathi and T. K. Varadan 1996 *Journal of Sound and Vibration* **192**, 1–14. Large amplitude vibrations of circular cylindrical shells.
5. A. W. Leissa 1973 *NASA SP-288, Vibration of Shells*. Washington, DC: U.S. Government Printing Office.
6. L. H. Donnell 1938 *Proceedings of the 5th International Congress on Appled Mechanics*. A discussion of thin shell theory.
7. K. M. Mushtari 1938 *Izv. Fiz. Mat. Ob-va. Pri Kaz. Un-te*. **11**, 8. Certain generalisations of the theory of thin shells (in Russian).
8. A. E. H. Love 1888 *Philosophical Transactions of the Royal Society of London, Series A* **179**, 491–549. The small free vibrations and deformations of a thin elastic shell.
9. S. Timoshenko 1959 Theory of Plates and Shells. New York: McGraw-Hill.
10. E. Reissner 1941 *American Journal of Mathematics* **63**, 177–184. A new derivation of the equations of the deformation of elastic shells.
11. P. M. Naghdi and J. G. Berry 1964 *Journal of Applied Mechanics* **21**, 160–166. On the equations of motion of cylindrical shell.
12. V. Z. Vlasov 1964 *NASA TTF-99*. General theory of shells and its application in engineering (English transl.).
13. J. L. Sanders 1959 *NASA TR-R24*. An improved first approximation theory for thin shells.
14. R. Byrne 1944 *Seminar Reports in Mathematics, University of California Publication in Mathematics, N.S*, Vol. 2, 103–152. Theory of small deformations of a thin elastic shell.
15. W. Flügge 1934 *Statik und Dynamic der Schalen*. Berlin: Julius Springer.
16. A. L. Goldenveizer 1968 *Applied Mathematics Mechanic* **32**, 704–718. Method for justifying and refining the theory of shells.
17. A. I. Lur'ye 1940 *Prikladnaya Matematika i Mekhanika* **4**, 7–34. General theory of elastic shells.
18. V. V. Novozhilov 1964 *The Theory of Thin Elastic Shells*. (Groningen, The Netherlands): P. Noordhoff Lts.
19. A. W. Leissa 1984 *Proceedings of the Second International Conference on Recent Advances in Structural Dynamics* 262–272. Non-linear analysis of plates and shell vibrations.

20. R. BENAMAR, M. M. K. BENNOUNA and R. G. WHITE 1989 *Proceedings of the Seventh International Modal Analysis Conference, Las Vegas, Nevada, U.S.A.* Non-linear mode shapes and resonance frequencies of fully clamped beams and plates.
21. R. BENAMAR, M. M. K. BENNOUNA and R. G. WHITE 1991 *Journal of Sound and Vibration* **149**, 179–195. The effects of large vibration amplitudes on the mode shapes and natural frequencies of thin elastic structures. Part I: simply supported and clamped–clamped beams.
22. M. M. BENNOUNA and R. G. WHITE 1984 *Journal of Sound and Vibration* **96**, 309–331. The effects of large vibration amplitudes on the fundamental mode shape of a clamped–clamped uniform beam.
23. A. H. NAYFEH and S. A. NAYFEH 1994 *Journal of Vibration and Acoustics* **116**, 129–136. On non-linear modes of continuous systems.
24. H. N. CHU 1961 *Journal of the Aerospace Sciences* **28**, 602–609. Influence of large amplitudes on flexural vibrations of thin circular cylindrical shells.
25. H. H. BLEICH and M. L. BARON 1954 *Journal of Applied Mechanics* **21**, 178–184. Tables for frequencies and modes of free vibration of infinitely long thin cylindrical shells.
26. M. L. BARON and H. H. BLEICH 1954 *Journal of Applied Mechanics* **21**, 167–177. Free and forced vibration of an infinitely long cylindrical shell in an infinite acoustic medium.
27. G. COUPRY 1962 *La recherche Aeronautique* **91**, 60–65. Vibrations de respiration des cylindres minces. Hommogènes ou non.
28. M. K. AU-YANG 1978 *Journal of Sound and Vibration* **57**, 341–355. Natural frequencies of cylindrical shells and panels in vacuum and in a fluid.
29. R. N. ARNOLD and G. B. WABURTON 1949 *Proceedings of the Royal Society of London Series A* **197**, 238–256. Flexural vibrations of the walls of thin cylindrical shells having freely supported ends.
30. S. B. DONG 1968 *Journal of the Acoustical Society of America* **44**, 1628–1635. Free vibration of laminated orthotropic cylindrical shells.
31. G. B. WARBURTON and J. HIGGS 1970 *Journal of Sound and Vibration* **11**, 335–338. Natural frequencies of thin cantilever cylindrical shells.
32. J. B. GREENSBERG and Y. STAVSKY 1980 *Acta Mechanica* **36**, 5–29. Buckling and vibration of orthotropic composite cylindrical shells.
33. H. E. WILLIAMS 1992 *Journal of Sound and Vibration* **15**, 277–288. On free vibration of thin cylindrical shells with large circumferential wave-number: Rayleigh's solution.
34. K. M. LIEW and K. C. HUNG 1995 *International Journal of Solids and Structures* **32**, 3499–3513. Three-dimensional vibratory characteristics of solid cylinders and some remarks on simplified beam theories.
35. K. M. LIEW, K. C. HUNG and M. K. LIM 1995 *Journal of Applied Mechanics* **62**, 718–724. Vibration of stress-free hollow cylinders of arbitrary cross section.
36. K. C. HUNG, K. M. LIEW and M. K. LIM 1995 *Acta Mechanica* **113**, 37–52. Free vibration of cantilevered cylinders: effects of cross-sections and cavities.
37. K. M. LIEW, K. C. HUNG and M. K. LIM 1997 *Journal of Sound and Vibration* **200**, 505–518. Three-dimensional vibration analysis of solid cylinders of polygonal cross-section using the *p*-Ritz method.
38. K. M. LIEW, C. W. LIM and S. KITIPORNCHAI 1997 *Applied Mechanics Reviews* **50**, 431–444. Vibration of shallow shells: a review with bibliography.
39. E. REISSNER 1955 *Report No. AM*5-6, *Guided Missile Research Division, The Ramo-Wooldrigge Corp., September* 30. Non-linear effects in the vibrations of cylindrical shells.
40. M. AMABILI, F. PELLICANO and M. P. PAÏDOUSSIS 1998 *Journal of Fluid and Structures* **12**, 883–918. Non-linear vibrations of simply supported circular cylindrical shells coupled to quiescent fluid.
41. D. A. EVENSEN 1968 *American Institute of Aeronautics and Astronautics Journal* **7**, 1401–1403. Non-linear vibrations of infinitely long cylindrical shell.
42. A. W. LEISSA 1973 *NASA SP*-288, *Vibration of Shells*, 220–222. Washington, DC: U.S. Government Printing Office.
43. E. H. DOWELL and C. S. VENTRES 1968 *International Journal of Solids and Structures* **4**, 975–991. Modal equations for the non-linear flexural vibration of a cylindrical shell.
44. D. A. EVENSEN 1966 *Journal of Applied Mechanics* **33**, 553–560. Non-linear flexural vibrations of thin circular rings.
45. J. H. GINSBERG 1973 *Journal of Applied Mechanics* **40**, 471–477. Large amplitude forced vibrations of simply supported thin cylindrical shells.

46. S. ATLURI 1972 *International Journal of Solids and Structures* **8**, 549–569. A perturbation analysis of non-linear free flexural vibrations of a circular cylindrical shell.
47. G. C. SINHARAY and B. BANERGEE 1985 *International Journal of Non-linear Mechanics* **20**, 69–78. Large amplitude free vibrations of shallow spherical shell and cylindrical shell—a new approach.
48. Y. KOBAYACHI and A. W. LEISSA 1995 *International Journal of Non-linear Mechanics* **30**, 57–66. Large amplitude free vibration of thick shallow shells supported by shear diaphragms.
49. K. K. RAJU and G. V. RAO 1976 *Journal of Sound and Vibration* **44**, 327–333. Large amplitude asymmetric vibrations of some thin shells of revolution.
50. T. UEDA 1979 *Journal of Sound and Vibration* **64**, 85–95. Non-linear free vibrations of conical shells.
51. R. BENAMAR 1990 *Ph.D. Thesis, University of Southampton*. Non-linear dynamic behaviour of fully clamped beams and rectangular homogeneous and laminated plates.
52. R. BENAMAR, M. M. K. BENNOUNA and R. G. WHITE 1993 *Journal of Sound and Vibration* **164**, 295–316. The effects of large vibration amplitudes on the mode shapes and natural frequencies of thin elastic structures. Part II: fully clamped rectangular isotropic plates.
53. R. BENAMAR, M. M. K. BENNOUNA and R. G. WHITE 1990 *Proceeding of the Fourth International Conference on Recent Advances in Structural Dynamics, Southampton*. The effects of large vibration amplitudes on the mode shapes of a fully clamped, symmetrically laminated, rectangular plates.
54. F. MOUSSAOUI and R. BENAMAR 1998 *6ème Colloque Maghrébin sur les Modèles Numériques de l'Ingénieur*. The effect of large vibration amplitudes on the mode shapes and natural frequencies of an isotropic elastic circular cylindrical shells of infinite length.
55. F. MOUSSAOUI, R. BENAMAR and R. G. WHITE 1999 *Vibration, Noise and Structural Dynamics*, vol. 1, The effect of large vibration amplitudes on the mode shapes and natural frequencies of simply supported thin elastic circular cylindrical shells.
56. F. MOUSSAOUI, R. BENAMAR and R. G. WHITE 2000 *Journal of Sound and Vibration* **232**, 917–943. The effect of large vibration amplitudes on the mode shapes and natural frequencies of thin elastic shells. Part I: coupled transverse–circumferential mode shapes of isotropic circular cylindrical shells of infinite length.
57. M. AMABILI, F. PELLICANO and M. P. PAÏDOUSSIS 2001 *Journal of Sound and Vibration* **243**, 182–183. Comment on "The effect of large vibration amplitudes on the mode shapes and natural frequencies of thin elastic shells. Part I: coupled ….".
58. F. MOUSSAOUI, R. BENAMAR and R. G. WHITE 2001 *Journal of Sound and Vibration* **243**, 184–189. Authors' reply.
59. A. W. LEISSA 1973 *NASA SP*-288, *Vibration of Shells* 37–43. Washington, DC: U.S. Government Printing Office.
60. R. D. BLEVINS 1984 *Formulas for Natural Frequency and Mode Shape*, 296–297. Florida: Kriger publishing Company.
61. M. J. D. POWELL 1965 *Computer Journal* **7**, 303–307. A method for minimising a sum of squares of non-linear functions without calculating derivatives.

APPENDIX A

The purpose of this appendix is to justify the approximation made in the present paper, according to which it may be assumed, when the motion is predominately transverse, that:

$$c_n = -nb_n$$

in which n is the order of the shell free mode of vibration considered, b_n and c_n are the coefficients of the circumferential and transverse displacements functions $(\sin(ny/R))$ and $(\cos(ny/R))$ respectively. This assumption will be justified both in the linear and non-linear cases on the light of previously published results.

A.1. THE LINEAR CASE

According to the results which are considered as classical, corresponding to the coupled transverse–circumferential vibration of thin elastic shells of infinite length, published in the monograph of Leissa [59, 60], the coefficients b and c defined above are related from the

TABLE A1

Percentage error in linear case for the first four modes

Mode ordern (n)	Lowest frequency from Reference [59]	$\frac{b}{c} = \frac{n}{\omega_l^{*2} - n^2}$	$\frac{b}{c} = -\frac{1}{n}$	Error (%)
1	$1{\cdot}02062 \times 10^{-2}$	$-1{\cdot}0001042$	$-1{\cdot}000$	0·0104
2	$5{\cdot}16417 \times 10^{-2}$	$-0{\cdot}5003336$	$-0{\cdot}500$	0·0334
3	$1{\cdot}23256 \times 10^{-1}$	$-0{\cdot}3338970$	$-0{\cdot}333$	0·0564
4	$2{\cdot}21118 \times 10^{-1}$	$-0{\cdot}2507663$	$-0{\cdot}250$	0·0766

single-mode approach to

$$b/c = n/(\omega_l^{*2} - n^2). \tag{A.1}$$

in which ω_l^{*2} is the lowest frequency parameter associated with the mode considered, and correspondg to a motion which is predominately transverse. It should be noticed that a typographic mistake occurred in the monograph (p. 42), in which one can read n^2 and $\Omega^2 - n^2$ instead of n and $n^2 - \Omega^2$ in equation (2.32) of reference [59].

In Table A1 are given the values of the ratio b/nc obtained from equation (A.1), in which n varies from 1 to 4 (which corresponds to the modes considered in the present paper) and ω_l^* is replaced by the values given in Table 2.2 of reference [59] for the associated lowest frequencies of an infinite long shell having $\beta = h/R = 0{\cdot}05$. It can be seen in Table A1 that the error induced by taking $b/nc = 1$, which is the approximation made in the present work, does not exceed 0·1%.

A.2. NON-LINEAR CASE

In Part I [56] of this series of paper, the first and second coupled transverse–circumferential non-linear mode shapes have been determined for a wide range of vibration

TABLE A2

Percentage error in non-linear case

(a) First mode $\omega_l^{*2}/\omega_{nl}^{*2}$ [56]	C_1 [56]	B_1 [56]	C_1/B_1	Error (%)
1·00087	0·0500	$-0{\cdot}0500$	$-1{\cdot}00000$	0·0000
1·10207	0·5500	$-0{\cdot}5501$	$-0{\cdot}99982$	0·0180
1·27698	0·9500	$-0{\cdot}9502$	$-0{\cdot}99979$	0·0210
1·68759	1·6500	$-1{\cdot}6510$	$-0{\cdot}99939$	0·0610
1·95233	2·0500	$-2{\cdot}0510$	$-0{\cdot}99951$	0·0488
(b) second mode $\omega_l^{*2}/\omega_{nl}^{*2}$ [56]	C_2 [56]	B_2 [56]	$C_2/2B_2$	Error (%)
1·00217	0·05	$-0{\cdot}02502$	$-0{\cdot}99932$	0·0680
1·25867	0·55	$-0{\cdot}27529$	$-0{\cdot}99895$	0·1053
1·66939	0·95	$-0{\cdot}47588$	$-0{\cdot}99815$	0·1849
2·38985	1·65	$-0{\cdot}82815$	$-0{\cdot}99620$	0·3804
2·74853	2·05	$-1{\cdot}03020$	$-0{\cdot}99495$	0·5048

amplitudes. Although a multi-mode approach was adopted in this work for both the transverse displacement W and the circumferential displacement V, which were expanded as series of six functions, the predominant terms for all amplitudes considered were B_1 and C_1 for the first mode, and B_2 and C_2 for the second mode. Also, it was found, as may be seen in Table A2(a, b), that C_1/B_1 may be approximated by unity with a percentage error not exceeding 0·1%, and that $C_2/2B_2$ may be approximated by unity with a percentage error not exceeding 0·5%.

APPENDIX B: NOMENCLATURE

V_b, V_a, V	bending, axial and total strain energy respectively
T	kinetic energy
y	circumferential position co-ordinate
h	shell thickness
R	radius of shell median surface
E	Young's modulus
D	bending stiffness
ρ	mass density per unit volume
β	thickness to radius ratio
$\mathbf{k}_{ij}$, $\mathbf{m}_{ij}$, $\mathbf{b}_{ijkl}$	general term of the rigidity tensor, the mass tensor and the non-linear tensor respectively
$\mathbf{k}^*_{ij}$, $\mathbf{m}^*_{ij}$ and $\mathbf{b}^*_{ijkl}$	general term of the non-dimensional rigidity tensor, mass tensor and non-linearity tensor respectively
$W(y,t)$	transverse displacement at point y of the shell $W(y,t) = w(y)\cos\omega t$
ω_{nl}, ω^*_{nl}	frequency and non-dimensional frequency parameter respectively
$\{\mathbf{C}\}$	column matrix $\{\mathbf{C}\}^{\mathrm{T}} = [c_1, \ldots, c_n]$
[**K**], [**M**], [**B**]	rigidity, mass and non-linearity matrices, respectively
σ, σ^*	stress and non-dimensional stresses respectively
*	the star exponent indicates non-dimensional parameters